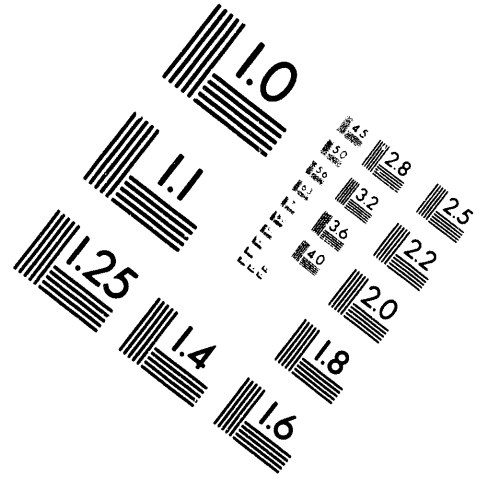
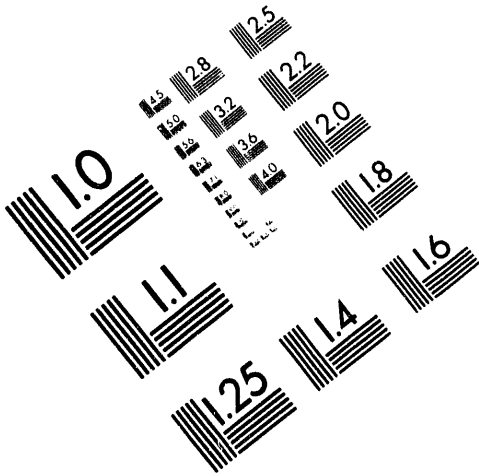




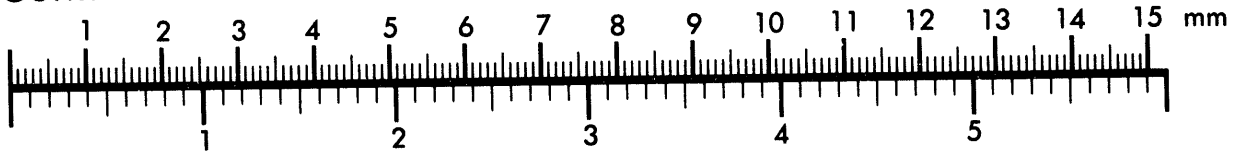
AIM

Association for Information and Image Management

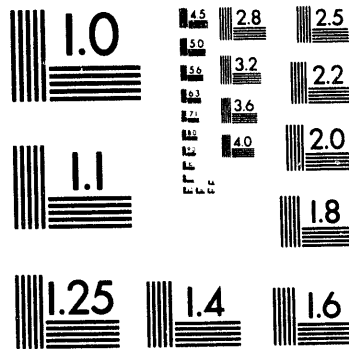
1100 Wayne Avenue, Suite 1100
Silver Spring, Maryland 20910
301/587-8202



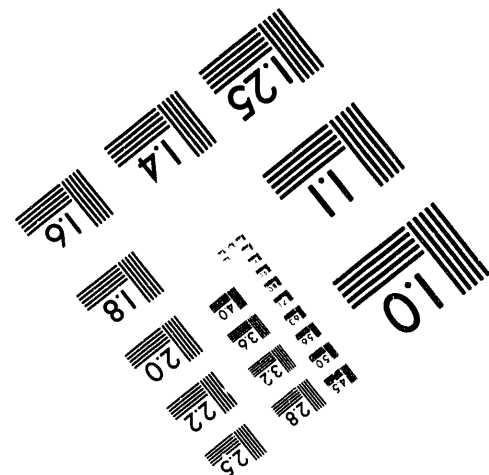
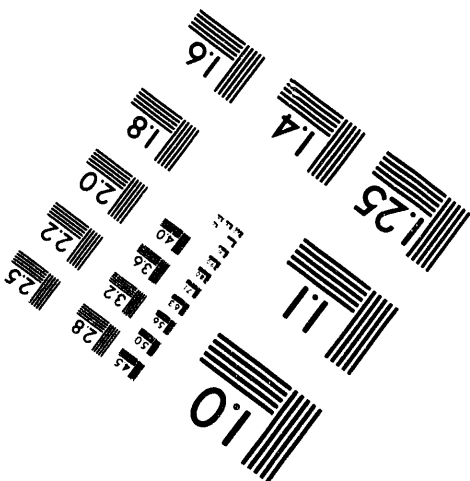
Centimeter



Inches



MANUFACTURED TO AIM STANDARDS
BY APPLIED IMAGE, INC.



1 of 1

*Actinide(IV) and Actinide(VI)
Carbonate Speciation Studies by
PAS and NMR Spectroscopies*

*Yucca Mountain Project
Milestone Report 3031-WBS 1.2.3.4.1.3.1*

*David L. Clark
Scott A. Ekberg
David E. Morris
Phillip D. Palmer
C. Drew Tait*

DISTRIBUTION OF THIS DOCUMENT IS UNLIMITED

for

MASTER

Table of Contents

	Page
i. List of Figures	vi
ii. List of Tables	vii
iii. Glossary of Acronyms	viii
1. Actinide Speciation: A Multifaceted Spectroscopic Approach	2
2. Photoacoustic Spectroscopic Studies of Pu(IV) Speciation in Carbonate Media	8
2.1 Introduction	8
2.2 Experimental Procedures	9
2.3 Results and Discussion	10
2.4 Concluding Remarks	23
3. Carbon-13 Nuclear Magnetic Resonance Kinetic Study of Carbonate Exchange on Plutonyl(VI) Carbonate Complexes.	25
3.1 Introduction	25
3.2 Experimental Procedures	28
3.3 ¹³C NMR of the Plutonium(VI) Carbonate System	30
3.4 Kinetic Data Treatment	34
3.5 Mechanism of Carbonate Exchange	43
3.6 Concluding Remarks	48
4. Acknowledgment	51
5. References	52
6. Quality Assurance Documentation	62

List of Figures

Figure	Title	Page
Figure 1.1.	The multifaceted spectroscopic approach to determine radionuclide speciation in solution.	7
Figure 2.1.	Photoacoustic absorption spectra (PAS) of 1 mM Pu(IV) and 1.0 M total carbonate as a function of pH.	12
Figure 2.2.	PAS of 1 mM Pu(IV) in 0.10 M Na ₂ CO ₃ and in 3 mM NaHCO ₃ .	14
Figure 2.3.	PAS of 250 nM Pu(IV) at pH between 8.4 and 8.9 as a function of bicarbonate concentration ranging from 0.6, 0.4, 0.2, and 0.1 M.	15
Figure 2.4.	PAS of colloidal Pu(IV) particles, with total plutonium 24 ppm by weight.	18
Figure 2.5.	Effect of Pu(IV) concentration on speciation at 0.4 M total carbonate concentration and pH between 8.4 and 9.	20
Figure 2.6.	Kinetic effect on 50 nM Pu spectra.	21
Figure 2.7.	Temperature dependence for 1.0 mM Pu(IV) at 0.4 M NaHCO ₃ and pH = 9.17.	22
Figure 2.8.	pH / total carbonate concentration predominance diagram.	24
Figure 3.1.	The basic structural unit of AnO ₂ (CO ₃) ₃ ⁴⁻ .	27
Figure 3.2.	62.9 MHz ¹³ C NMR spectra for solutions containing 99.9% ¹³ C-enriched ²⁴² PuO ₂ (CO ₃) ₃ ⁴⁻ and free carbonate.	33
Figure 3.3.	The influence of chemical exchange on the line width, Δν _{1/2} , of an NMR signal as a function of temperature.	37
Figure 3.4.	A typical ¹³ C NMR spin-echo relaxation experiment following the free carbonate resonance.	39
Figure 3.5.	Eyring plots for the plutonyl tris carbonate system at plutonium concentrations listed.	45
Figure 3.6.	Proposed mechanism for carbonate self-exchange on actinyl tris carbonate complexes in aqueous solution.	50

List of Tables

Table	Title	Page
Table 3.1.	Compositions of the Solutions investigated by ^{13}C NMR.	31
Table 3.2.	T_2 Spin-echo data for free carbonate.	40
Table 3.3.	Plutonyl Carbonate Sample 1 Data.	41
Table 3.4.	Plutonyl Carbonate Sample 2 Data.	42
Table 3.5.	Plutonyl Carbonate Sample Data Corrected to 1M Concentration.	46
Table 3.6.	Comparison of activation parameters for actinyl triscarbonate systems.	47

Glossary of Acronyms

CPMG	Carr-Purcell-Meiboom-Gill NMR Pulse Sequence
DOE	United States Department of Energy
EQ3/6	Equilibrium Thermodynamic Modeling Code
EXAFS	Extended X-ray Absorption Fine Structure
LIF	Laser Induced Fluorescence
NHE	Normal Hydrogen Electrode
NIR	Near Infra Red
NMR	Nuclear Magnetic Resonance
PAS	Photoacoustic Spectroscopy
PZT	Lead Zirconate Titanate
SCE	Saturated Calomel Electrode
XAS	X-ray Absorption Spectroscopy
YMP	Yucca Mountain Site Characterization Program

Actinide(IV) and Actinide(VI) Carbonate Speciation Studies by PAS and NMR Spectroscopies

Yucca Mountain Project
Milestone Report 3031-WBS 1.2.3.4.1.3.1

by
David L. Clark, Scott A. Ekberg, David E. Morris,
Phillip D. Palmer, and C. Drew Tait

ABSTRACT

Pulsed-laser photoacoustic spectroscopy (PAS) and Fourier-transform nuclear magnetic resonance (NMR) spectroscopy have been employed to study the speciation of actinide(IV) and actinide(VI) ions (Np, Pu, and Am) in aqueous carbonate solutions as a function of pH, carbonate concentration, actinide concentration, and temperature. The PAS study has focused exclusively on Pu(IV) speciation. The stability fields on a pH (8.4 to 12.0) versus total carbonate concentration (0.003 to 1.0 M) plot for dilute Pu(IV) carbonate species ($[Pu]_{tot} = 1 \text{ mM}$) have been mapped out using photoacoustic spectroscopy. Four different plutonium species, characterized by absorption peaks at 486, 492, 500, and 512 nm have been found. In contrast to previously reported results (Eisworth et al. 1985), loss of a single carbonate ligand likely does not account for the difference in speciation for the two species associated with the 486 and 492 nm absorption peaks, nor can any of the observed species be identified as colloidal Pu(IV). The effects of variations in total Pu(IV) concentration suggest that polynuclear plutonium species may be present in the solutions. NMR data have been obtained for UO_2^{2+} , PuO_2^{2+} and AmO_2^{2+} in aqueous carbonate solutions. This report focuses on results for PuO_2^{2+} . The ligand exchange reaction between free and coordinated carbonate on the $PuO_2(CO_3)_3^{4-}$ systems has been examined by variable temperature ^{13}C NMR spectroscopic techniques. In each of the six different $PuO_2(CO_3)_3^{4-}$ samples examined, two NMR signals are present, one for the free carbonate ligand and one for the carbonate ligand coordinated to a paramagnetic plutonium metal center. The single ^{13}C resonance line for coordinated carbonate is consistent with expectations of a monomeric $PuO_2(CO_3)_3^{4-}$ species in solution. A modified Carr-Purcell-Meiboom-Gill NMR pulse sequence was used for experimental determination of ligand exchange parameters for paramagnetic actinide complexes. Eyring analysis at standard conditions provided activation parameters of $\Delta H^\ddagger = 38 \text{ KJ/M}$ and $\Delta S^\ddagger = -60 \text{ J/K}$ for the plutonyl triscarbonate system, suggesting an *associative* transition state for the plutonyl(VI) carbonate complex self-exchange reaction.

1. Actinide Speciation: A Multifaceted Spectroscopic Approach

The determination of solution speciation of actinides and other radionuclides that will comprise the radioactive inventory of a high-level nuclear waste repository under site-specific conditions is an important component in the Yucca Mountain Site Characterization Program to demonstrate the efficacy of solubility and sorption as barriers to the transport of these radionuclides away from the engineered barrier system and into the accessible environment (DOE, 1988a and b). Speciation implies the specification of the oxidation state of the radionuclide, and the chemical structure of the inner-coordination sphere (i.e., the identity and number of coordinating ligands). By determining speciation, a description of the chemical equilibria and the formation constants that link the various radionuclide species is also obtained. In this way, it will be possible to utilize thermodynamic modeling codes [e.g., EQ 3/6 (Wolery, 1983; Wolery et al., 1989)] to predict radionuclide speciation and solubility under solution conditions for which these determinations are not being made empirically. For example, the present strategy for empirical determinations of radionuclide solubility calls for measurements using three to four groundwater compositions that should bracket the conditions expected at the proposed repository. An accurate description of speciation will enable interpolation of solubility between these bracketing groundwaters as well as extrapolation to other potentially unexpected groundwater compositions resulting from, for example, perturbations introduced from dissolution of components of the engineered barrier system or changes in global climate.

In the ensuing discussion, we will focus on speciation studies of the actinides because they are a major concern with respect to site-characterization activities for the proposed repository, and they represent the greatest experimental challenge. However, the discussion can be generalized to other radionuclides in the inventory (e.g., nickel, tin, and zirconium) that normally form complexes with inorganic and / or organic ligands and

therefore can exist under differing chemical forms as a function of groundwater composition.

Under most environmentally relevant conditions, actinide speciation is dominated by hydrolysis processes (e.g., complexation by H_2O , OH^- , and O^{2-}) with perturbations introduced by complexation with simple inorganic anions such as carbonate and phosphate (Baes and Mesmer, 1976; Allard, 1982; Martell and Smith, 1982). Traditionally, most actinide speciation studies have resorted to classical, non-spectroscopic methods such as potentiometry and / or multiphase extraction to elucidate the chemical equilibria in these systems, because these methods are sensitive to the inherent Brønsted acid / base properties of the actinide species. Unfortunately, the applicability of these classical methods is generally inadequate because (1) the concentration limits for the actinides are extremely low under near-neutral pH conditions resulting in extremely small changes in the experimental observable (e.g., pH), and (2) the complexity of the speciation for highly hydrolyzed species renders the interpretation ambiguous. It is now recognized that the best speciation information is generally provided by spectroscopic methods that can probe speciation directly. However, even spectroscopic methods can suffer from the two limitations outlined above. The key to effective use of spectroscopic methods for speciation is to implement a combination of three to four differing techniques that complement each other in such a way that these limitations are overcome.

The YMP Speciation Task at Los Alamos has identified four complementary spectroscopic methods that are being implemented for actinide speciation studies. The cornerstone technique is pulsed-laser photoacoustic spectroscopy (PAS). This technique is rapidly gaining acceptance as the premiere method for determining actinide speciation in solution (Bennett et al., 1992; Berg et al., 1991a and b; Beitz et al., 1990; Okajima et al., 1990; Klenze and Kim, 1988; Beitz et al., 1988; Pollard et al., 1988; Eiswirth et al., 1985; Stumpe et al., 1984). The theoretical and experimental bases for the technique have been

summarized in a number of review publications (Patel and Tam, 1981; Tam, 1986). In short, this technique provides the functional equivalent of an electronic or vibrational absorption spectrum. The principal advantage of PAS is its extreme sensitivity. We and others have shown that actinide electronic absorption spectra can be obtained for solutions having total actinide concentrations of $\sim 10^{-9}$ moles/liter (Bennett et al., 1992; Berg et al., 1991 a and b; Beitz et al., 1990; Okajima et al., 1990). For many actinides in near-neutral solutions, this is at or near the solubility limit. Therefore, PAS affords the opportunity to obtain spectral data on speciation under solution conditions comparable to those found in environmental groundwaters. A related technique, laser-induced fluorescence spectroscopy (LIF), is based on the same theoretical principles and provides even better sensitivity than PAS. However, LIF is applicable only to luminescent actinides, of which Am^{3+} is the only probable candidate of importance to YMP.

While PAS and LIF afford the advantage of direct interrogation of speciation under the extremely dilute actinide concentrations expected in Yucca Mountain groundwaters, they provide this speciation information only implicitly. That is, the information on actinide oxidation state(s) and coordinating ligand environments is encoded in the electronic spectral data. To specify speciation in an unambiguous way, spectroscopic techniques are needed that provide explicit information on molecular structure. Two such techniques are being implemented in the Speciation Task. The first is multinuclear Fourier-transform nuclear magnetic resonance spectroscopy (NMR). The application of this technique to actinide speciation has been documented in several recent publications (Strom et al., 1981; Aberg et al., 1983a and b; Ferri et al., 1988). NMR spectra provide readily interpretable information on the identity and number of coordinating ligands and their disposition about the actinide ion(s) in the species. The second explicit technique is synchrotron-based x-ray absorption spectroscopy (XAS). Here, too, recent reports have documented the applicability of XAS to actinide speciation (Combes et al., 1992). The theoretical

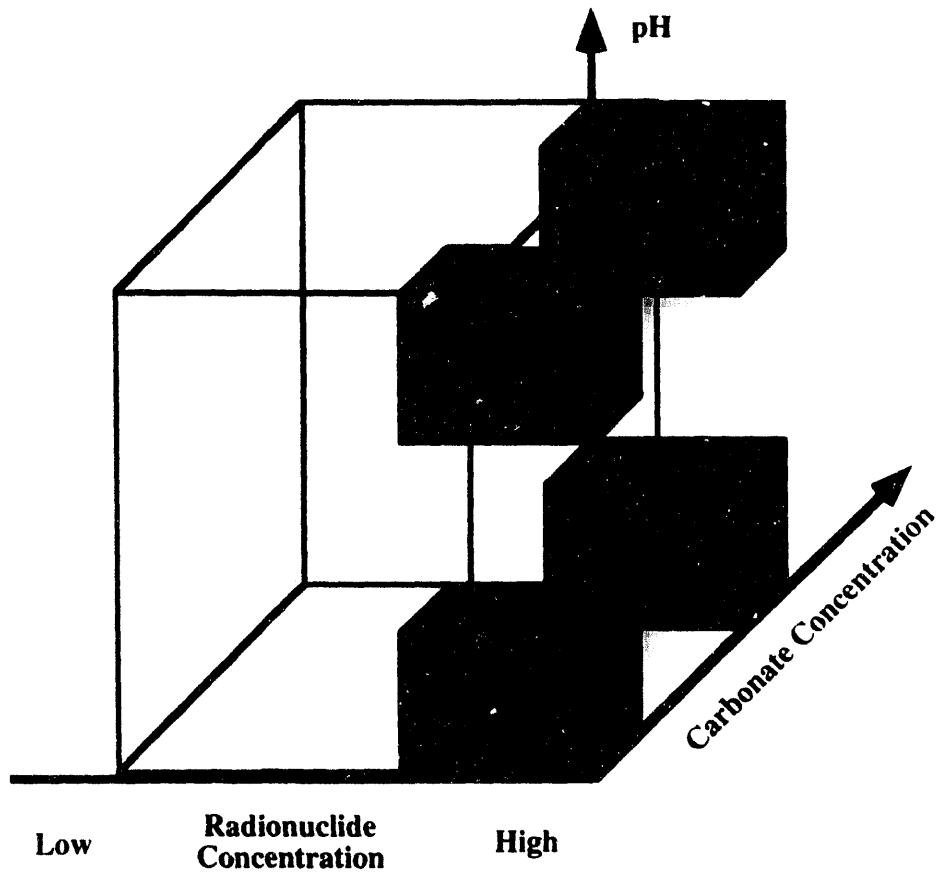
underpinnings of XAS are described by Koningsberger and Prins (1988). This technique provides a direct measure of the oxidation state of the actinide from the energy of the absorption edge. It also provides a snap-shot of the local chemical structure with a level of detail and precision comparable to that provided from x-ray diffraction, but for solution species as well as solids.

Both NMR and XAS provide the explicit chemical structural information necessary to unambiguously specify speciation. However, the sensitivities of these methods are much lower than PAS and LIF. For most applications, NMR and XAS are applicable in the actinide concentration range of 10^{-3} to 10^{-6} moles / liter. In most cases, this concentration range exceeds the solubility limit of the actinides in typical groundwaters. This does not limit the applicability and value of these techniques, however, because experimental strategies can be devised to take advantage of the complementarity of NMR and XAS with respect to the more sensitive PAS and LIF methods. One such strategy is illustrated in Figure 1.1. In essence, the less sensitive methods are used to establish speciation cornerstones. The spectral signatures for these cornerstone structures are then obtained using the more sensitive PAS and /or LIF probes. Having thereby established the link between speciation and spectroscopic signature for the cornerstone species, the more sensitive methods can be used to probe speciation over a broad range of solution conditions to map out speciation and equilibria more thoroughly.

In this report, preliminary data are presented for Pu(IV) speciation in carbonate media using PAS spectroscopy (Chapter 2), and for Pu(VI) [as PuO_2^{2+}] speciation in carbonate media using ^{13}C NMR spectroscopy (Chapter 3). The Pu(IV) carbonate system was chosen for our initial work because it is the least well understood of all the oxidation states of plutonium, and the interpretation of spectroscopic data in previous reports on Pu(IV) carbonate speciation (Eiswirth et al., 1985) seems inconsistent. In addition, we have been concerned about the reported low relative abundance of the tetravalent oxidation

state compared to the penta- and hexavalent states of plutonium in the steady-state solutions resulting from the solubility studies in Well J-13 and UE25p#1 waters (Nitsche et al., 1987a and b; 1992a-c). The initial NMR studies have concentrated on the hexavalent oxidation states of the actinides in carbonate media, in large part because there are existing literature reports (Strom et al., 1981; Aberg et al., 1983a and b; Ferri et al., 1988) on the use of this technique on the chemically similar hexavalent uranium (uranyl, UO_2^{2+}) system. These existing data have served as a calibrant for the application of the technique to the more challenging neptunium, plutonium, and americium systems. In addition, very recent results suggest that plutonyl (PuO_2^{2+}) species are prevalent in the steady-state solutions from solubility experiments using water from Well UE25p#1 (Nitsche et al., 1992d).

The results presented in this report fall short of a complete implementation of our multifaceted spectroscopic approach. However, these results do demonstrate the accomplishment of an important intermediate goal in route to the implementation of our ultimate strategy. Namely, we have successfully applied an implicit technique (PAS) and an explicit technique (NMR) to germane actinide speciation problems. Our next goal is to bring together the explicit and implicit structural techniques on a single, important speciation problem to provide unambiguous molecular structure and thermodynamic data. The most probable system for this purpose is Np(V)O_2^+ in carbonate media, because this actinide ion has the highest solubility (Nitsche et al., 1992 a-d) of any of the transuranic ions likely to be encountered in groundwaters at the repository site, and it is thought to be only poorly sorbing on typical soils and minerals.






- 
High Concentration Regime: Explicit Speciation from NMR and XAS
- 
Low Concentration Regime: Implicit Speciation from PAS and LIF
- 
Overlap Concentration Regime: Molecular Structure / Spectral Signature Correlation is Established by Explicit and Implicit Methods for Inter- / Extrapolation to Other Solution Conditions

Figure 1.1. The multifaceted spectroscopic approach to determine radionuclide speciation in solution.

2. Photoacoustic Spectroscopic Studies of Pu(IV) Speciation in Carbonate Media

2.1 Introduction

To understand the possible migration/retention of nuclear wastes from a potential long-term repository in the event of water infiltration (a worst-case scenario), solubility and sorption studies of transuranic elements such as plutonium must be undertaken. Ultimately, bulk solubility and sorption characteristics derive from molecular-level considerations of actinide speciation, which includes inner-sphere coordination and nucleation (i.e. possible polymeric species) as well as valence state. Speciation studies have had a long-standing history in inorganic chemistry for a wide variety of solution complexes such as transition metal cations, and extension to the transuranics is a natural progression from classical inorganic chemistry.

To be relevant for radionuclide repository issues, a realistic choice of actinide and potential ligand must be made. Plutonium is a significant product in spent nuclear fuel, and from considerations of standard oxidation potentials and hydrolysis reactions, plutonium(IV) could be an important valence state under pH and Eh conditions expected for natural groundwaters (Hobart, 1990; Choppin and Stout, 1991). As relevant potential ligands, carbonates have been studied because they are expected to be readily available, either as leachates from cement enclosures of a radioactive waste repository or from natural groundwaters (Stumm and Morgan, 1985; Lindsay, 1979; Baes and Mesmer, 1976). The total carbonate concentration, mostly as bicarbonate, of Well J-13 water taken from Yucca Mountain, Nevada has been measured at 118 - 143 mg/liter \approx 2 mM (Ogard and Kerrisk, 1984). Paleozoic water from the deeper UE-25p#1 well tapping a carbonaceous aquifer under Yucca Mountain contains an order of magnitude more carbonate (Ogard and Kerrisk, 1984), and further shows the importance of these carbonate dependent studies. Therefore,

detailed knowledge of Pu(IV)-carbonate speciation is needed to predict migration/retention characteristics of plutonium.

To that end, speciation-sensitive absorption bands in the electronic spectra of actinides can be used to monitor actinide changes with environment (Carnall and Crosswhite, 1989). Actinide visible absorptions are dominated by f-f transitions (Carnall and Crosswhite, 1989; Fred, 1989), and although f-electrons are generally shielded from covalent interactions and hence produce very sharp spectra, the spectra do shift with electrostatic changes induced by changes in speciation. However, for these weak parity-forbidden f-f bands to be observed under conditions approaching environmental relevance (near neutral pH, radionuclide concentrations in the tens of nanomolar range), sensitive techniques such as pulsed photoacoustic absorption spectroscopy [PAS (Patel and Tam, 1981; Tam, 1986)] must be employed. In this chapter, we report our results from such PAS experiments on dilute Pu(IV) carbonate. While the exact identity of the Pu complexes giving rise to the absorption peaks studied here are not known, this study does map-out predominance regions of interest. Future studies from more structure-specific (but less sensitive) techniques such as NMR, EXAFS, and X-ray crystallography may subsequently allow us to match these optical absorbance signals with definite complexes.

2.2 Experimental Procedures

A stock of 1.4 mM $^{242}\text{Pu(IV)}$ in 3.00 M sodium carbonate solution served as our actinide source. The Pu stock was made by first dissolving [as Pu(III)] the pure metal in 6M HCl, followed by electrolytic oxidation at 1.2 V vs. NHE as described elsewhere (Newton et al., 1986a). Conventional UV/Vis spectroscopy (Perkin Elmer Lambda 9) was used to confirm sample integrity during the course of the experiments (~ 1 year). The ^{242}Pu isotope is about 15.5 times less radioactive than ^{239}Pu and 4400 times less active than ^{238}Pu and allowed us to work outside of glove boxes. Sodium carbonate (J.T. Baker,

'Baker Analyzed' reagent grade) and sodium bicarbonate (Mallinckrodt, analytical reagent grade) were used as received. Solutions were filtered with 1 micron Acrodisc CR PTFE syringe filters, and the pH was measured with an ORION model 290-A meter and a ROSS combination electrode.

The pulsed photoacoustic instrument used here will be described in detail elsewhere. The third harmonic (355 nm) from a 10 Hz Nd/YAG Q-switched laser (Quanta-Ray DCR-3) was used to pump a dye laser (Quanta-Ray PDL-2) with Coumarin 460, 480, or 500 laser dye (Exciton, Inc). The 5 ns output pulse (at 6 mJ/pulse) was focused just beyond a stoppered 2.0 cm quartz cell containing the filtered plutonium sample. The spectral signal resulted from a shock wave produced by excited-state energy dissipation from an absorbing species, where the shock wave intensity is proportional to the absorbance at a particular wavelength. A spectrum was composed from multiple readings (typically 640 laser shots) at each successive wavelength. The shock wave was converted to an electrical signal by a shielded piezoelectric transducer (PZT) crystal, and amplified / filtered by two cascaded Stanford Research Systems SR560 amplifiers (x200 each). The signal was further filtered with two 10th order high pass, 1st order low pass passive filters described by Beitz et al. (1990) [bandpass from 100 kHz to 1.3 MHz] and read by a digital oscilloscope (Hewlett-Packard 54111D). The wave was digitally rectified and the PAS signal integrated. The precision in the readings is represented by the ± 2 standard deviation of the mean (95% confidence level) error bars. The data presented are single-beam spectra. References (water + (bi)carbonate blank, measured under the same conditions and cells as the sample spectra) were subtracted from the Pu spectra.

2.3 Results and Discussion

The initial impetus for this work was a previous study (Eisworth et al., 1985) exploring speciation changes of Pu(IV) carbonates versus pH using optical spectroscopies.

Specifically, this report alleged that three species ($[\text{Pu}(\text{CO}_3)_5]^{6-}$, $[\text{Pu}(\text{CO}_3)_4]^{4-}$, and $[\text{Pu}(\text{CO}_3)_3]^{2-}$) were found between $\text{pH} = 12$ and $\text{pH} = 8$, based on their fit to data at 425, 444, 474, and 485 nm. However, only two peaks (486 and 492 nm) were resolved in the electronic absorption spectra from 470 to 500 nm, and a pH dependent plot of $\epsilon(425)$, $\epsilon(444)$, and $\epsilon(474)$ vs. $\epsilon(488)$ is linear, also indicating only two species. However, the concentration of plutonium was different at each pH, varying from 120 mM at high pH to 1 mM at $\text{pH}=8$ (saturated solutions were used throughout). To test whether two or three species were actually present, we systematically changed pH with constant $[\text{Pu}]$ and constant total carbonate (i.e. constant $[\text{CO}_3^{2-}] + [\text{HCO}_3^-]$) to look for the presence or absence of an isobestic point in the absorption spectra. The results of this experiment are summarized in Fig. 2.1. The 1 mM Pu(IV) concentration was chosen because it was the lowest concentration used in the previous study (Eisworth et al., 1985) and therefore avoided the possibility of precipitation. For an idea of the optical densities involved, note that the extinction coefficient of this peak has been measured previously to be $\sim 90 \text{ cm}^{-1}\text{M}^{-1}$ in 1 M sodium bicarbonate solution (Wester and Sullivan, 1983), so the absorbance at 486 nm in Fig. 2.1 would be 0.00018. In fact, only the 486 nm peak is observed throughout the range studied. This implies the presence of only one species, in marked contrast to previous reports (Eisworth et al., 1985; Kim et al., 1983). These previous studies proposed that the species associated with the 486 nm peak is $[\text{Pu}(\text{CO}_3)_5]^{6-}$, but other corroborative evidence may be necessary before making this a definite assignment.

To pursue this surprising result and to try to reconcile our study with the previous ones, we varied the concentration of total carbonate while keeping the pH relatively constant. At high pH ($\text{pH} = 11.3$), the 486 nm peak is replaced with one at 500 nm as the carbonate concentration is changed from 1.0 to 0.1 M (Fig. 2.2). However, because such

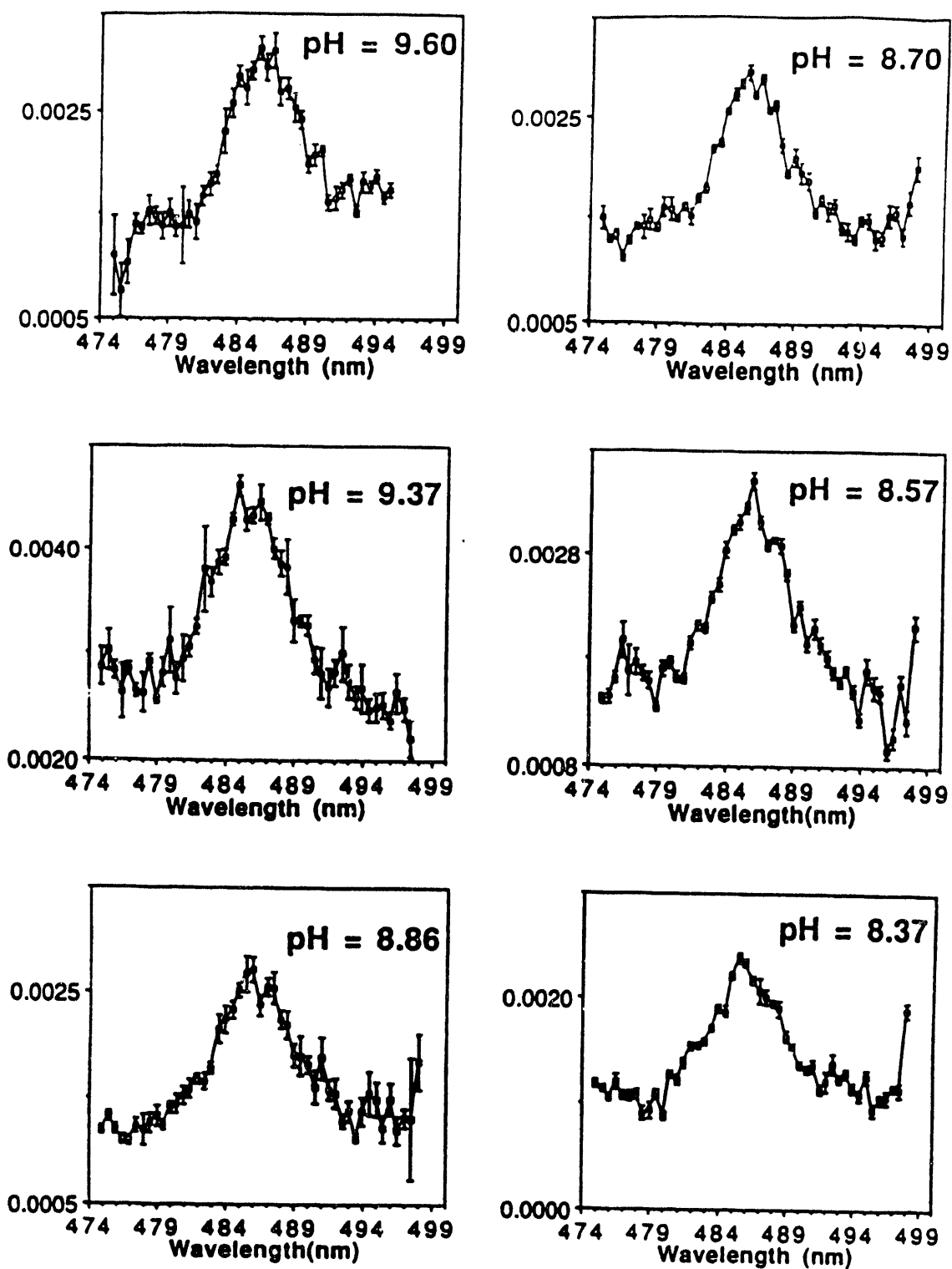
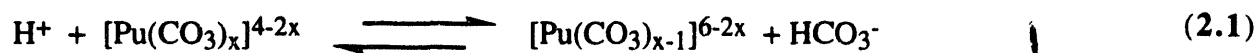


Figure 2.1. Photoacoustic absorption spectra (PAS) of 1 mM Pu(IV) and 1.0 M total carbonate as a function of pH.

high pH's are unlikely in a repository or natural environment, we have focused on pH's in the 8.5 range, dominated by free bicarbonate anions. Fig. 2.3 shows the effect of changing the (bi)carbonate concentration from 1.0 to 0.1 M. Despite the small pH changes, the solution $[\text{HCO}_3^-]/[\text{CO}_3^{2-}]$ ratio is at least 25 (at pH=8.9 with a pK_a of 10.3) and is therefore predominately bicarbonate throughout. The previously reported (Eisworth et al., 1985) 492 nm peak is apparent, arising from a change in total bicarbonate present. A third species associated with 12 and 3 mM bicarbonate concentrations was marked by no absorbance peak in the wavelength range shown in Fig. 2.3, but did show a feature at 513 nm (Fig. 2.2b). Generally, a red shift (486 --> 492 --> 513 nm) is exhibited with decreasing bicarbonate concentration. Note that these changes occur over small ranges of bicarbonate concentrations. If the changes were due to simple carbonate dissociation, the following equilibrium expressions could be written:



$$\frac{[\text{Pu}(\text{CO}_3)_x]^{4-2x}}{[\text{Pu}(\text{CO}_3)_{x-1}]^{6-2x}} = \frac{[\text{HCO}_3^-]}{[\text{H}^+]\text{K}} \quad (2.2a)$$

$$\frac{[\text{Pu}(\text{CO}_3)_x]^{4-2x}}{[\text{Pu}(\text{CO}_3)_{x-1}]^{6-2x}} = \text{K}'[\text{HCO}_3^-] \quad (2.2b)$$

The spectra show that the ratio on the left hand side of equation (2.2b) changes from ~10:1 (almost total dominance by the 486 nm peak) to ~1:10 (almost total dominance by the 492 nm peak, leading to a total change of a factor of 100) over a bicarbonate concentration change of less than one log unit (i.e. a factor of 10). Therefore, $[\text{HCO}_3^-]$ raised to a mere power of 1 (as shown in equation 2.2b) can not account for the data, and hence the loss of one carbonate can not account for the data. Besides dissociation of more than one carbonate ligand, other possibilities include mixed

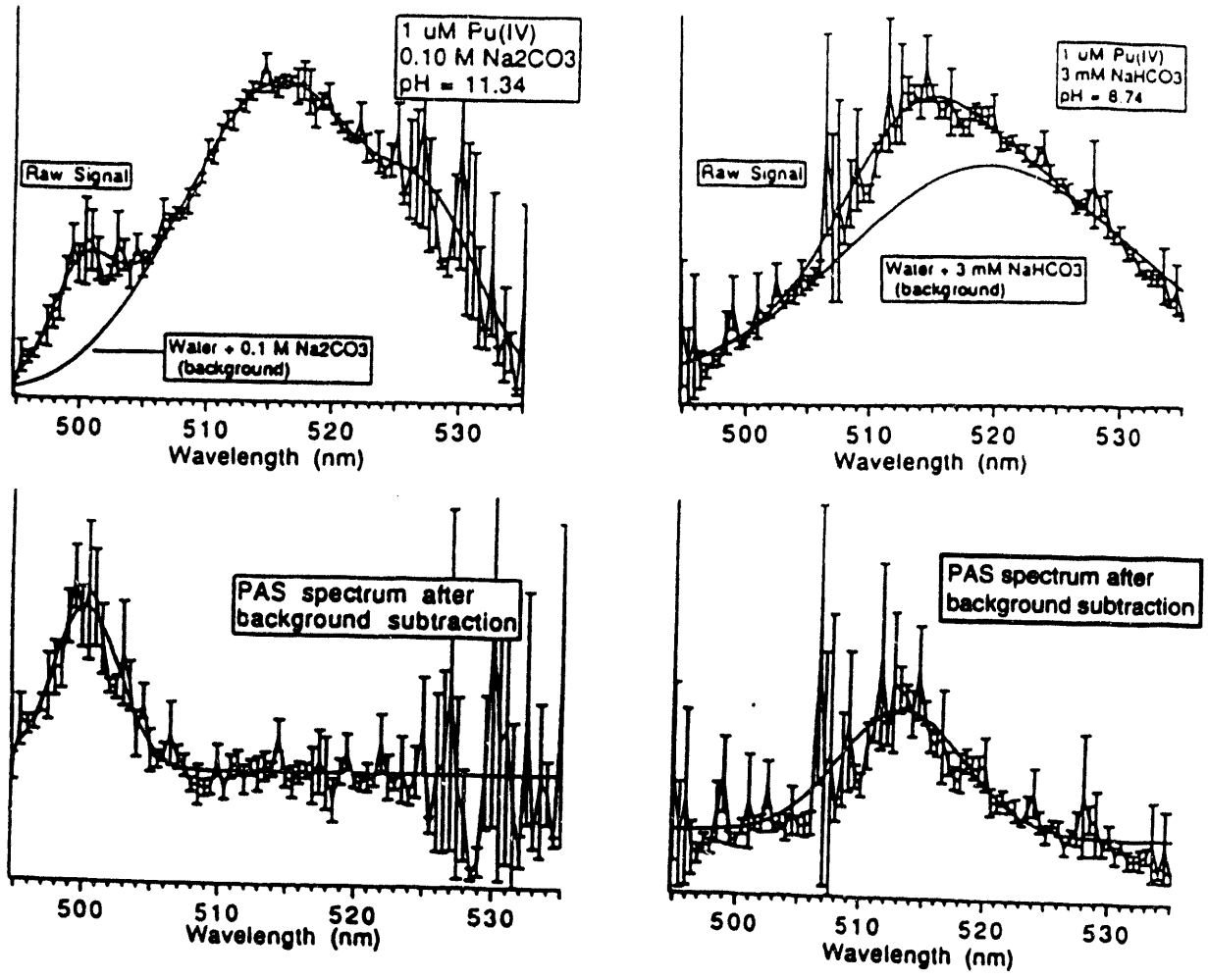


Figure 2.2. PAS of 1 mM Pu(IV) in 0.10 M Na₂CO₃ (a and b) and in 3 mM NaHCO₃ (c and d). Spectra a and c are raw single channel spectra which include water/carbonate backgrounds as well as the plutonium signal. Spectra b and d represent background subtracted spectra. The parameters for the background fit were set from separate experiments with only water and (bi)carbonate (i.e., no Pu) present.

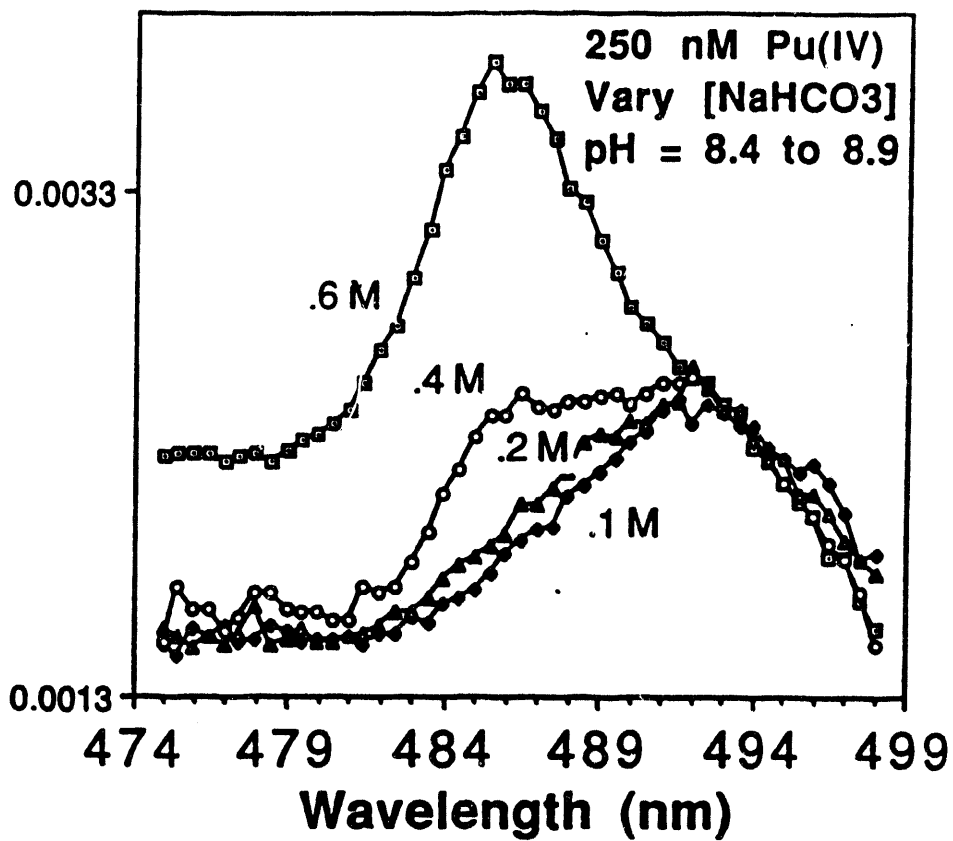


Figure 2.3. PAS of 250 nM Pu(IV) at pH between 8.4 and 8.9 as a function of bicarbonate concentration ranging from 0.6, 0.4, 0.2, and 0.1 M as indicated. Under these dilute conditions, no Pu precipitation is expected.

$\text{OH}^-/\text{CO}_3^{2-}$ complexes, replacement by bicarbonate, and cluster / colloid formation.

An interesting effect observed in Fig. 2.3 involves the lower PAS intensity of the 492 nm peak relative to the one at 486 nm. To demonstrate that the species represented by the 492 nm peak is not merely precipitating out of solution to produce a lower PAS signal, this set of experiments was performed at 250 nM Pu concentration. With Well J-13 water (pH=8.5, total carbonate concentration = 2 mM), plutonium solubility has been measured at 290 nM (Nitsche et al., 1992c). Consequently, no plutonium is expected to precipitate at 250 nM at pH \approx 8.5 and total carbonate concentration \geq 3 mM, and this argues against simple precipitation as the cause of the peak intensity change. From Fig. 2.3, the 492 nm peak may always be present at $[\text{HCO}_3^- + \text{CO}_3^{2-}] \geq 30$ mM but becomes masked by the strong 486 nm peak that appears at $[\text{HCO}_3^- + \text{CO}_3^{2-}] \geq 200$ mM.

To determine whether any of the spectra measured above are from Pu(IV)-colloid, we examined the absorption spectrum of dilute *bona fide* Pu(IV)-colloid. Figure 2.4 shows the PAS spectrum of Pu(IV) colloid particles which matches those found for more concentrated samples (Hobart et al., 1989). While this spectrum is obtained at total plutonium concentration two orders of magnitude below those obtainable by conventional spectroscopy, the intensity of the band at 510 nm is still considerably weaker than those of the other Pu species discussed here. Therefore, both the relative weakness of the colloid PAS signal and the different peak positions argue against assigning any of the peaks observed in Figs. 2.1-2.3 to a Pu(IV) colloid, although other oligomeric species such as dimers and trimers can not be ruled out. Note, however, that colloid formation from the monomeric stock solution may be quite slow at these low Pu concentrations, and its eventual formation can not be ruled out at low carbonate (<.1M) concentrations. Another study conducted by the Dynamic Transport task of the Yucca Mountain Project at Los Alamos (Triay et al., 1991) found that Pu(IV) colloid under similar final conditions (pH=7.9, $[\text{HCO}_3^-]=2$ mM, total $[\text{Pu(IV)}]=100$ nM) appeared to retain the colloid structure

upon dilution of an originally concentrated (1 mM total Pu) stock colloid solution, while a long-term solubility study (Nitsche et al., 1992c) in J-13 water also noted considerable Pu(IV) colloid formation. Even for concentrated Pu solutions, (total [Pu]=10 mM), colloid formation can take up to a month to occur (Newton et al., 1986a and b). Note, however, that colloid formation can occur faster (Newton and Rundberg, 1984).

The relative weakness of the PAS signal from the Pu(IV) colloid is an interesting effect in and of itself, and may be related to (a) the observation that PAS signals only come from shallow surface depths (Patel and Tam, 1981; Tam, 1986) with many of the plutonium atoms too deep inside the colloid to contribute, (b) a long excited-state lifetime relative to the resonance frequency of the PZT detector, and/or (c) low amplitude vibrations spread-out over the entire colloid resulting in negligible heat transfer to solvent.

The effect of plutonium concentration on the equilibrium is shown in Fig. 2.5. Because of the low solubility of Pu in near neutral waters, experiments that directly probe speciation with as low a concentration as possible are necessary to mimic natural conditions. A red shift of the absorption at the expense of the 486 nm peak is noted at lower Pu concentrations. However, a kinetic effect in the evolution of the more dilute spectra, and subsequent non-Beer's Law behavior, is also observed (Fig. 2.6), and further study of dilute samples involving different sample preparations is under investigation. Note that the 25 nM Pu spectrum is the most dilute actinide sample spectrum yet presented, and is very close to allowing us to probe Pu speciation under dilute carbonate concentrations and pH values closer to 7, where the concentration may approach as little as 10 nM (Nitsche et al., 1992c). Furthermore, the concentration dependence of Pu speciation implies some oligomerization process: if all species were monomeric, no concentration dependence would be noted (e.g., eq. 2.2). Therefore, although a *bona fide* Pu(IV) colloid species is not formed within the time frame of the experiment, lowering the

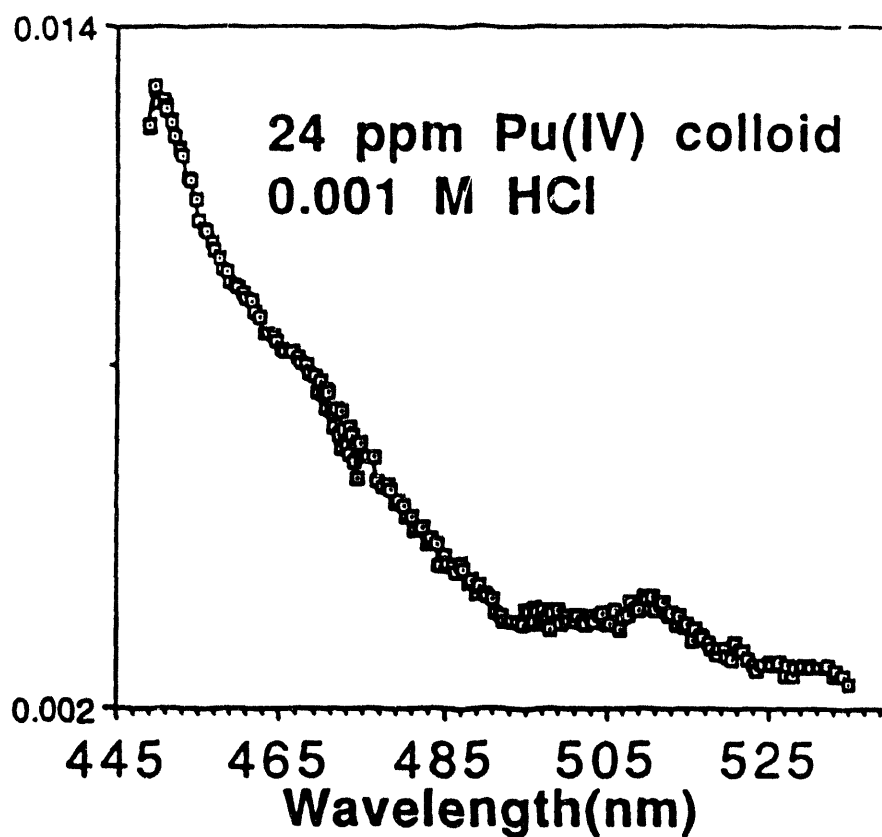


Figure 2.4. PAS of colloidal Pu(IV) particles, with total plutonium 24 ppm by weight. Following a previously determined recipe for colloid formation, the solution was made in 1 mM HCl. The spectrum consists of the overlap of three scans with laser dyes C460, C480, and C500.

carbonate concentration may result in the formation of species that have higher plutonium nuclearity (e.g., dimers, trimers, etc.).

Finally, we investigated the temperature dependence of the Pu-carbonate speciation at 0.4 M total carbonate, where speciation vs. [carbonate] is changing rapidly (see Fig. 2.3). Elevated temperatures are expected near any radionuclide repository due to the heating from released fission energy. Because the coefficient of expansion for water is larger at higher temperatures, the PAS signal should almost double over this temperature range (Patel and Tam, 1981; Tam, 1986; Beitz et al., 1990). The spectra in Figure 2.7 have not been corrected for this effect, and only relative changes should be noted. The 492 nm peak reversibly gains intensity relative to the 486 nm peak at higher temperatures. Many factors in addition to simple considerations based on LeChatlier's principle could be contributing to the observed reversible change in speciation with temperature manifested in these spectra. One important change related to solvent properties that would result in a reversible speciation change (i.e., a temperature dependence of the equilibrium constant between the species) is a decrease in the dielectric constant of water at elevated temperatures (Brimhall and Crerar, 1987; Seward, 1984). This lowered dielectric constant will destabilize a more highly charged species relative to one with a lower charge, consistent with carbonate loss from a highly coordinated complex. Entropic contributions from nuclearity changes could also be a factor, as $\Delta G = \Delta H - T\Delta S$ adds a temperature component to the equilibrium. However, due to changes in the solvent sphere that would accompany nuclearity change, even the overall sign of the DS term is difficult to estimate (Seward, 1984) and no inferences on nuclearity changes can be made.

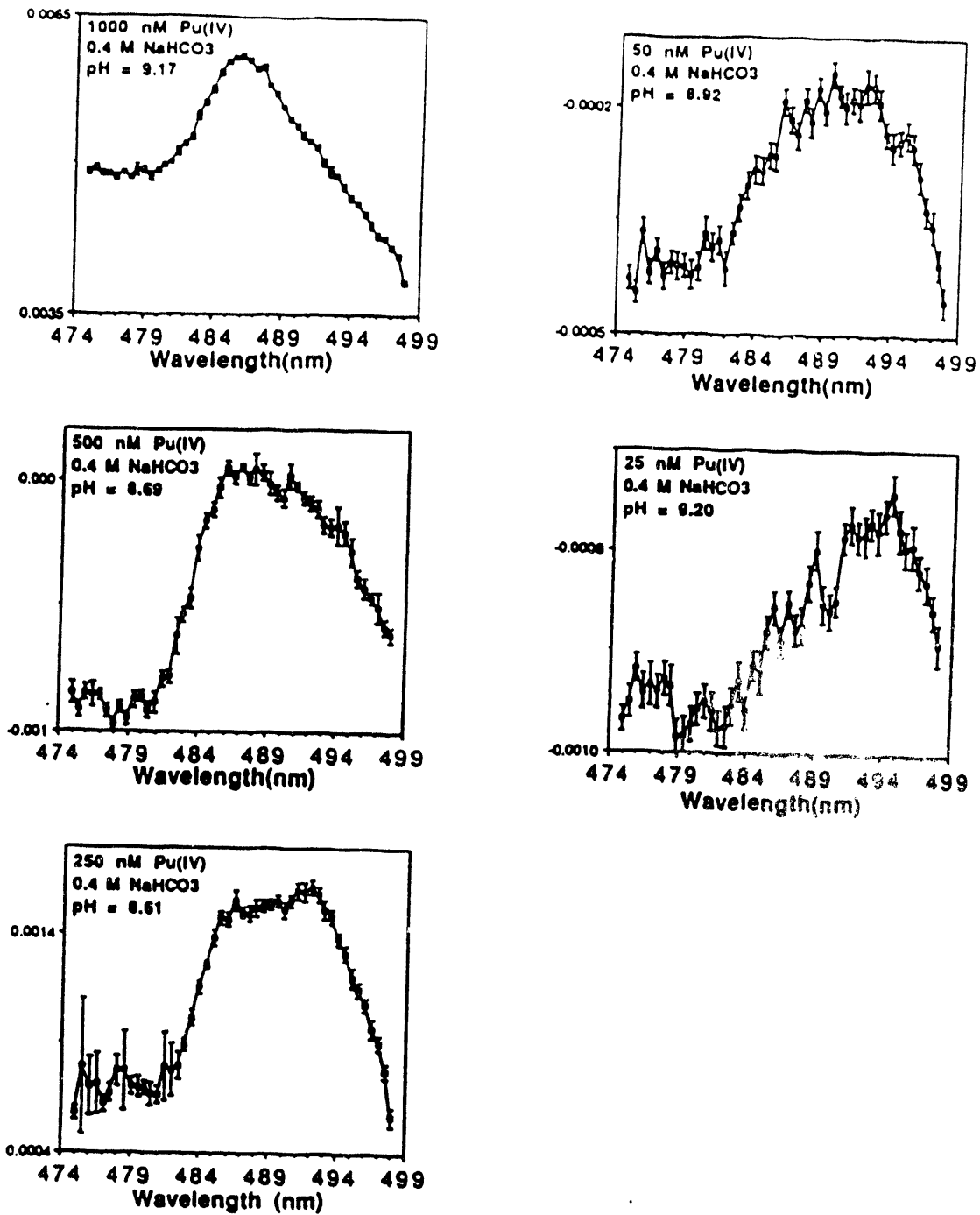


Figure 2.5. Effect of Pu(IV) concentration on speciation at 0.4 M total carbonate concentration and pH between 8.4 and 9 (pH and [Pu] are listed for each spectrum). Note that 25 nM Pu = 6 ppb by weight.

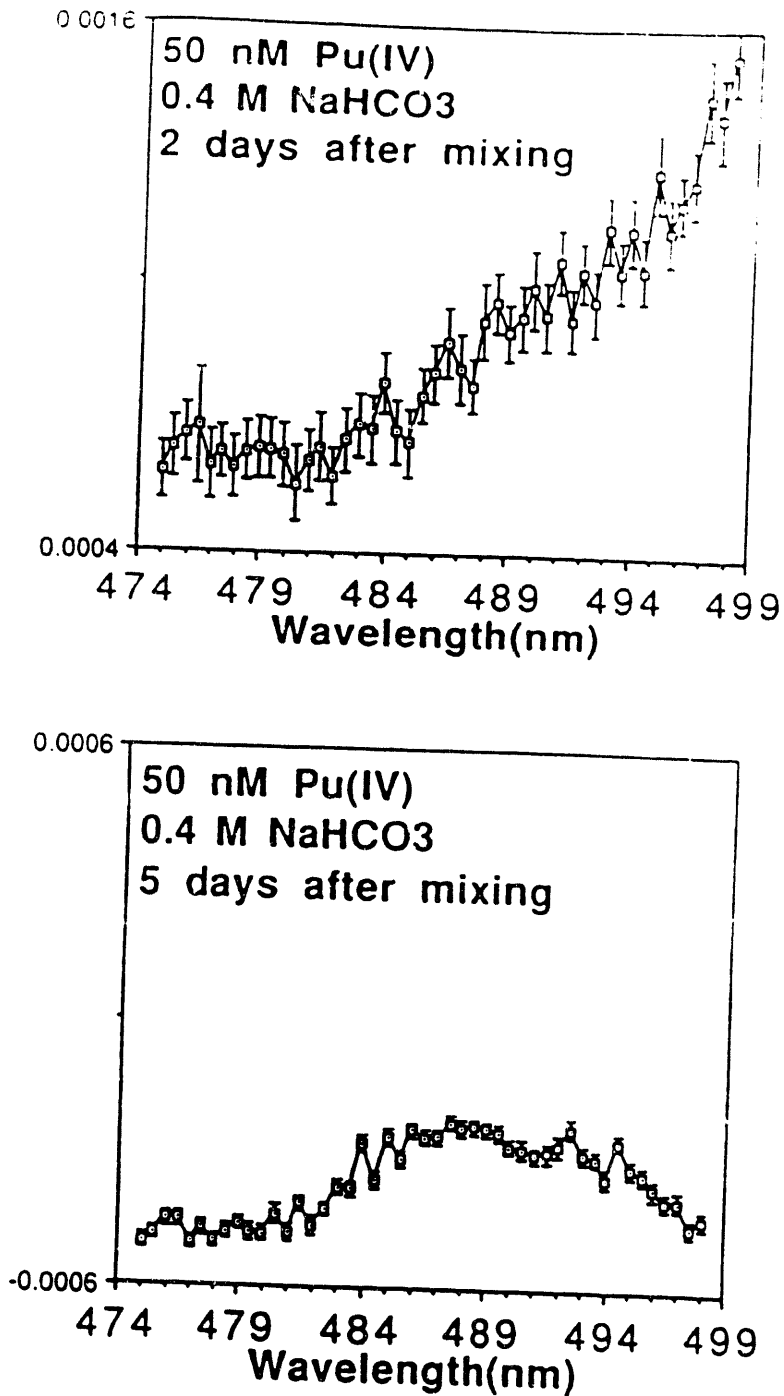


Figure 2.6. Kinetic effect on 50 nM Pu spectra shows that several days are required before a stable absorption spectrum is formed (2 days top spectrum, 5 days bottom spectrum). This effect is only evident for $[Pu] \leq 100$ nM.

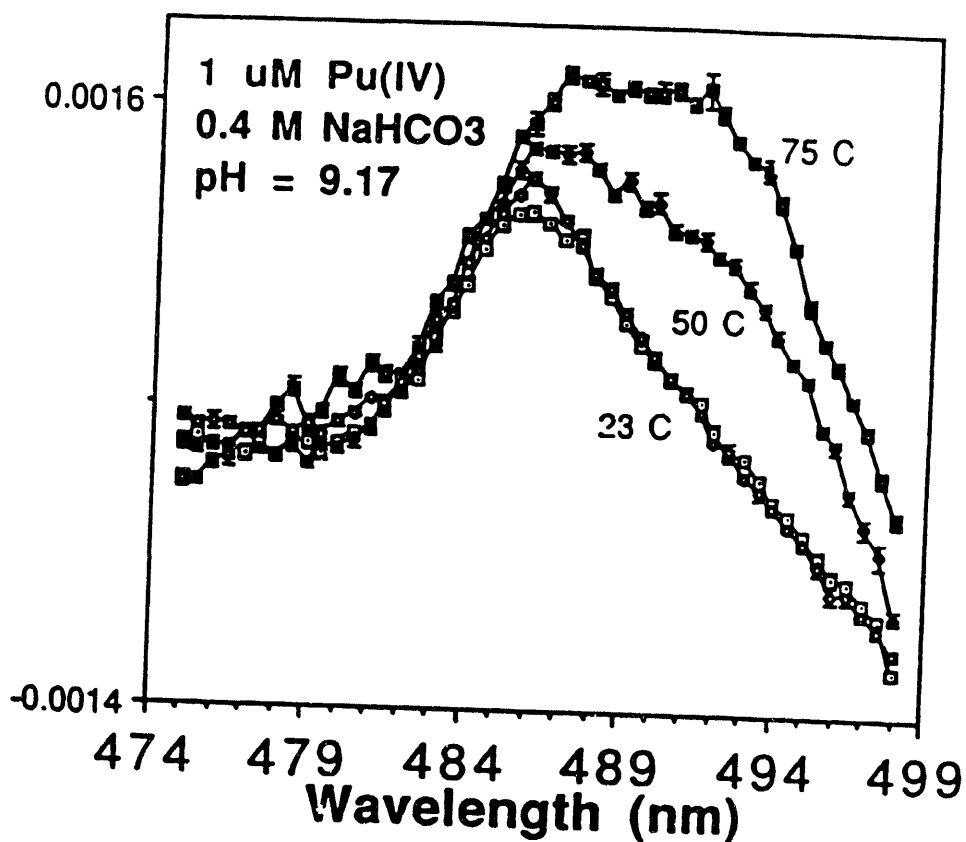


Figure 2.7. Temperature dependence for 1.0 mM Pu(IV) at 0.4 M NaHCO₃ and pH = 9.17. The relative intensity of the 486 nm peak diminishes with respect to the 492 nm peak at higher temperatures, indicating a change in the equilibrium constant between the species contributing to the spectra. This change is reversible: the same spectrum is found at 23°C before and after the temperature increase.

2.4 Concluding Remarks

In contrast to a previous report (Eiswirth et al., 1985), a single species with a 486 nm absorption signature is found to dominate in 1.0 M total carbonate solutions from pH 8.4 to at least pH 12. Other species with absorption peaks at 500 nm (0.1 M carbonate, pH=11), 492 nm (0.4 to 0.03 M bicarbonate, pH=8.5 to 9.0), and 513 nm (12 and 3 mM bicarbonate, pH=8.8) have been identified, and the room temperature stability field diagram is mapped-out in Fig. 2.8. The species with red-shifted spectra are associated with lower carbonate coordination to the Pu(IV) center, but the exact nature of these species is under investigation now at higher concentrations and complementary techniques such as NMR, XAS, and single-crystal x-ray diffraction. However, we can say that these new species are not simply due to the successive loss of single carbonate ligands, as the equilibrium reaction is not first order in (bi)carbonate. Lowering the concentration of Pu(IV) decreases the stability region dominated by the species giving rise to the 486 nm peak, but a kinetic effect still needs to be explored before this is understood. However, a nuclearity change is indicated. Finally, the species giving rise to the 486 nm peak may be highly charged, as judged from its reversible behavior at elevated temperatures and consistent with a high carbonate ligation field.

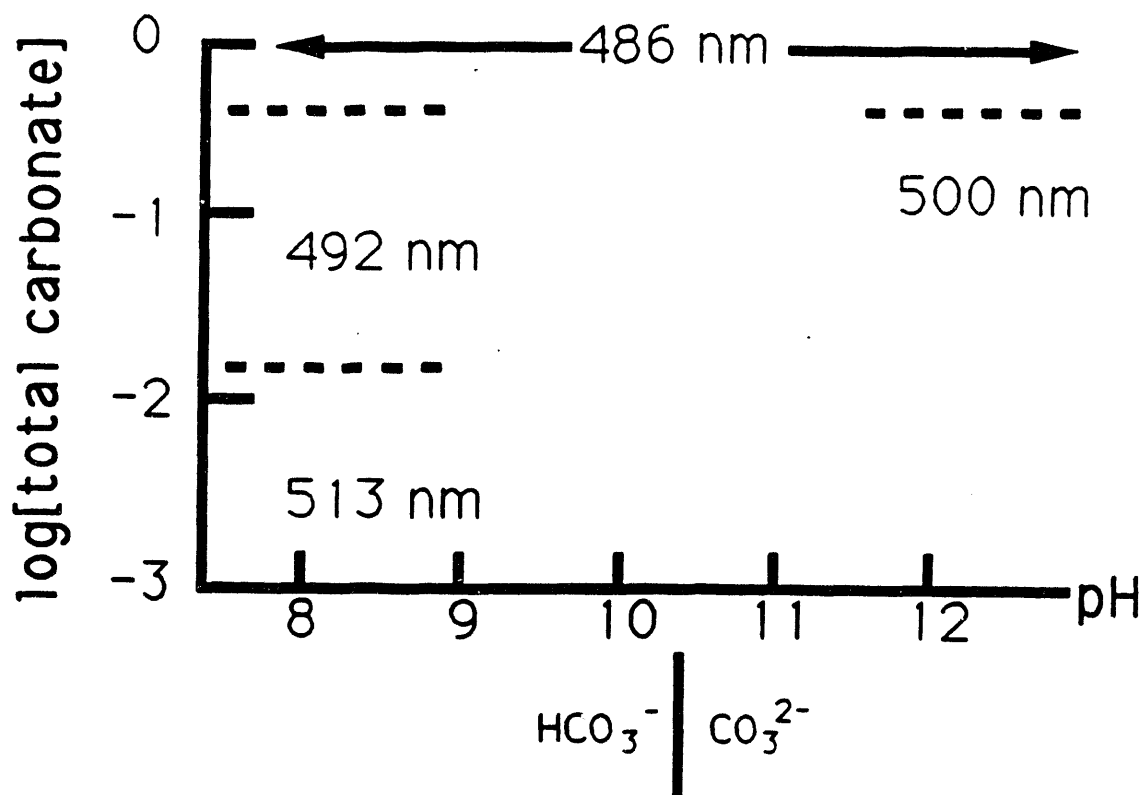


Figure 2.8. pH / total carbonate concentration predominance diagram showing regions of species dominance as determined from their diagnostic absorption peaks. Work is continuing with more structure-specific techniques such as EXAFS and NMR (but at higher concentration levels) to match the absorption peaks with definitive structures.

3. Carbon-13 Nuclear Magnetic Resonance Kinetic Study of Carbonate Exchange on Plutonyl(VI) Carbonate Complexes.

3.1 Introduction

The present chapter examines the feasibility of Nuclear Magnetic Resonance (NMR) as a tool for direct speciation studies of actinide ions in aqueous carbonate solutions. NMR spectroscopy is one of the most widely used physicochemical tools of investigation in the field of chemistry. Its obvious appeal derives from the possibility of directly monitoring nuclei of atoms that are located in strategic positions or are directly involved in chemical processes. NMR is a radiofrequency spectroscopic method based upon the quantized nuclear spin properties of nuclei with non-zero nuclear magnetic moments. Common examples of highly sensitive nuclei include ^1H , ^{13}C , ^{19}F , and ^{31}P . Hence, molecular structure determinations are commonly based upon NMR for organic, biological and inorganic compounds of importance in the chemical industry. Modern NMR methods are currently based upon Fourier-Transform signal accumulation, homogeneous field-superconducting magnets, and high speed computers for rapid data acquisition and manipulation.

Ions of the various actinide elements in the same oxidation state have very similar ionic radii. Thus it is reasonable to expect that chemical speciation will be similar across the series of early actinide elements (U, Np, Pu, Am) for a given oxidation state. The lanthanides and uranium are usually much easier to study than the transuranium elements, so chemical similarity is potentially very useful. However, data to check the quantitative validity of this concept are sparse. The comparative dynamic behavior of a series of actinyl ions AnO_2^{2+} (An = U, Np, Pu, Am) with a common carbonate ligand provides a unique opportunity to assess the relative importance of the variations in size and electronic

configuration on speciation and substitution reactions in solution, and thus the actinyl carbonate system was chosen as an ideal candidate to evaluate the utility of modern NMR techniques for direct speciation studies of actinide ions in carbonate solutions.

The structure and composition of the monomeric actinyl carbonate complex $AnO_2(CO_3)_3^{4-}$ is well established for uranium and neptunium. Figure 3.1 shows the solid state molecular structure of the anionic $UO_2(CO_3)_3^{4-}$ unit. The central actinide metal is surrounded by a hexagonal bipyramidal coordination polyhedron, with two apical oxygen atoms having An-O bond distances that are much shorter than the six equatorial An-O bonds. The equatorial coordination is formed with three bidentate carbonate ligands lying in the hexagonal plane as shown in Figure 3.1 (Coda et. al., 1981). Although the Np(VI), Pu(VI), and Am(VI) systems have not been as extensively studied as the U(VI) counterpart, several investigations indicate that the limiting complexes have the same stoichiometry as found in the uranium system in aqueous solutions containing three equivalents of carbonate or greater (Ullman and Schreiner, 1988; Ciavatta et. al., 1979). Solution Raman spectroscopic data are consistent with the maintenance of a linear O-An-O unit and bidentate carbonate ligands for $AnO_2(CO_3)_3^{4-}$ complexes in aqueous carbonate solutions for AnO_2^{2+} ions of U, Np, Pu, and Am. (Madic et. al., 1983; Basile et al., 1978). The existence of bicarbonate complexes of AnO_2^{2+} ions has not been demonstrated even in the pH ranges where bicarbonate ions are present in higher concentrations than carbonate (Maya, 1982).

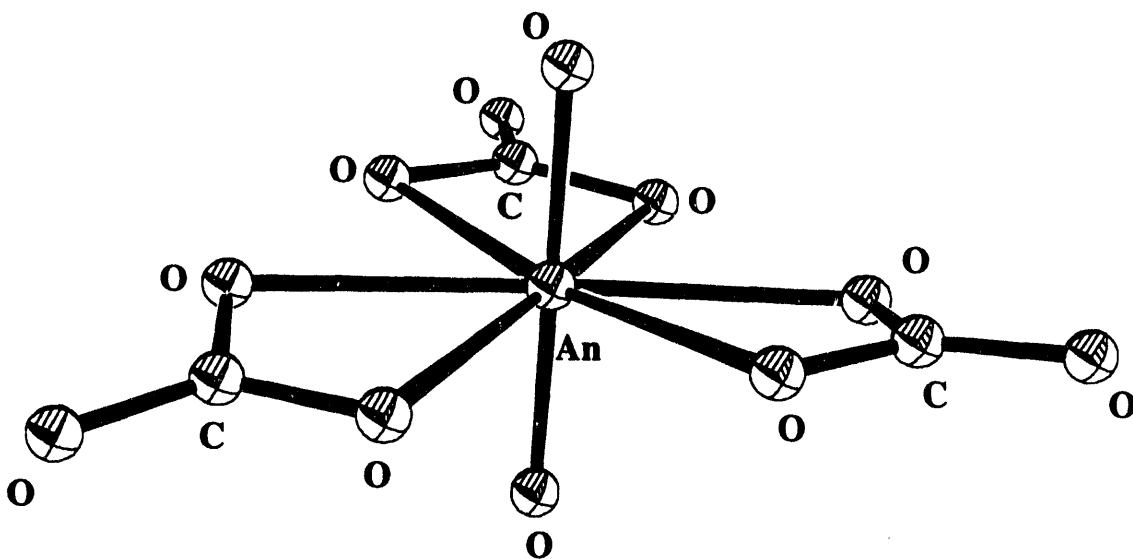


Figure 3.1. The basic structural unit of $AnO_2(CO_3)_3^{4-}$ emphasizing a hexagonal bipyramidal coordination geometry about the central actinide atom.

At present, there is not a great deal known about the kinetics of bidentate ligand exchange on actinyl(VI) complexes and there is disagreement in the primary literature with regards to the actual mechanism of carbonate self-exchange in this important actinyl triscarbonate system. Stout *et al.* (1992) reported exchange rate data for $\text{UO}_2(\text{CO}_3)_3^{4-}$ and $\text{NpO}_2(\text{CO}_3)_3^{4-}$ that suggested an associative transition state, while Brücher *et al.* (1991) reported data in support of a dissociative transition state. We have initiated an in-depth study of the carbonate self-exchange reaction (Equation. 3.1) on the corresponding $\text{PuO}_2(\text{CO}_3)_3^{4-}$ system by ^{13}C NMR, and our data helps to clear up the discrepancies noted above and sheds new light on the mechanism of carbonate exchange on this fundamentally important class of compound. Finally, our studies demonstrate that modern NMR spectroscopic techniques are directly applicable to paramagnetic actinide complexes and will undoubtedly have a significant impact in the areas of actinide speciation and solution chemistry kinetics.



3.2 Experimental Section

Spectrophotometric Measurements. Solution UV-visible-NIR spectra were recorded using a Varian CARY 17D spectrophotometer in matched 1.0 or 0.1 cm quartz cells. Extinction coefficients were measured from the baseline.

Electrochemical Preparations. The apparatus used in this study was an EG&G PAR Model 173 potentiostat / coulometer. The electrochemical cells used for bulk electrolysis had separate compartments for working, reference, and counter-electrodes and are described in detail elsewhere (Hobart *et. al.*, 1982). The working electrode was a Pt-screen; the counter electrode, a Pt wire, was separated from the experimental solution with a Vicor frit; and reference electrode was saturated calomel (SCE).

NMR Measurements. The NMR solutions were placed in Wilmad 4mm o.d. Teflon-FEP (Fluorinated Ethylene Propylene) NMR tube liners and sealed with a small soldering iron, then inserted into Wilmad 5mm o.d. 507-PP pyrex glass NMR tubes which were flame-sealed with a small hand torch. Variable temperature Fourier transform ^{13}C NMR spectra were recorded on a Bruker AF 250 spectrometer fitted with a selective probe head operating at 62.9 MHz with ^2H field lock. The $\pi/2$ pulse lengths were approximately 5.25 ms. The temperature was controlled with a Bruker variable temperature controller and was stable to within $\pm 1\text{K}$. The temperature was determined by measurement of the ^1H NMR of ethylene glycol (295 - 350 K) or methanol (270 - 295 K) at the same temperature and gas flow rate. The longitudinal relaxation rates of the free carbonate signal were measured by the inversion-recovery method to be 15 - 20 ms depending on concentration. Since it is very difficult to avoid field inhomogeneities in an NMR tube containing a highly paramagnetic actinide solution, we did not measure the full width at half-height ($\Delta\nu_{1/2} \approx 1/\pi T_2$) to determine the transverse relaxation rate (T_2), but instead we employed a modified Carr-Purcell-Meiboom-Gill pulse sequence (Carr and Purcell, 1954; Meiboom and Gill, 1958). The number of refocusing echoes was set to a constant value of 1, and the relaxation delay between the pulses was taken as a variable. All ^{13}C NMR chemical shifts are reported in ppm relative to the carbonyl carbon of acetone- δ_6 set at δ 206.0.

Materials and Solution Preparation. All of the common chemicals used were ACS Certified reagent grade and were used without further purification. Deuterium oxide (99.9 % D) and 99.9 % ^{13}C -enriched Na_2CO_3 were purchased from Cambridge isotopes. Deuterium oxide was degassed by bubbling nitrogen for 1 hr. $^{242}\text{PuO}_2$ (99.99%) was obtained from Los Alamos National Laboratory stock and purified as described in detail elsewhere (Newton et. al., 1986). A summary of this purification procedure is as follows. $^{242}\text{PuO}_2$ was dissolved in *conc.* HClO_4 and fumed to near-dryness. Distilled H_2O was added to the nearly-dry solid to bring the resulting Pu(VI) into solution. This solution was

electrolytically reduced to aquo Pu(III) in 1.5M HClO₄ using a conventional 3-electrode system at a potential of 0.75V (vs. NHE). The Pu(III) solution was subsequently electrochemically re-oxidized to Pu(IV) at about 1.2V (vs. NHE). At this potential, Pu(VI) is thermodynamically stable but its rate of formation is insignificant. Metallic impurities were removed using nitrate anion exchange. An equal volume of 16M HNO₃ was added to the form the nitrate complex, and this was loaded onto an anion exchange column (Lewatit MP-500FK, 40 - 70 mesh) which was pretreated with 8M HNO₃. The loaded column was washed several times with 8M HNO₃ and 9 M HCl to remove impurities, and then the purified Pu(IV) was eluted with 0.5M HCl. The resulting Pu(IV) solution was again fumed to near-dryness with an excess of conc. HClO₄ to regenerate PuO₂²⁺. The residue was brought back into solution with 2 mL of distilled H₂O, and assayed to be 1.1 M in Pu(VI) using the 831 nm absorbance measured on a Cary 17D UV-Vis-NIR spectrometer. A 2.0 M stock solution of Na₂¹³CO₃ in D₂O was prepared under nitrogen. ²⁴²PuO₂(¹³CO₃)₃⁴⁻ solutions were prepared by addition of the appropriate amount of Na₂¹³CO₃ / D₂O solution to the Pu(VI) stock solution (taking into account neutralization of acid) and adjusting the ionic strength with 4M NaClO₄ in D₂O. The UV-Vis-NIR spectrum from 400 - 1200 nm of each resulting solution was examined and found to be consistent with that previously reported for PuO₂(CO₃)₃⁴⁻. The composition of the resulting solutions is given in Table 3.1.

3.3 ¹³C NMR of the Plutonium(VI) Carbonate System

We have examined the PuO₂(CO₃)₃⁴⁻ system by employing variable temperature ¹³C NMR spin-echo relaxation techniques. Samples were isotopically enriched (99.9%) with labeled ¹³CO₃²⁻. A typical example of variable temperature ¹³C NMR spectral behavior for the ²⁴²PuO₂(¹³CO₃)₃⁴⁻ system is shown in Figure 3.2. The spectra shown in

Figure 3.2 reveals an experimental run that spans nearly 80°C, from which one can extract reliable kinetic data and activation parameters.

Table 3.1. Compositions of the Solutions investigated by ^{13}C NMR

Sample	1	2	3	4	5	6
$[\text{PuO}_2^{2+}]$	0.20	0.10	0.20	0.20	0.18	0.20
$[\text{CO}_3^{2-}] + [\text{HCO}_3^-]$	1.10	0.95	0.90	0.70	0.64	1.00
$[\text{ClO}_4^-]$	1.0	1.0	1.0	1.0	1.0	1.0
pH	9.48	10.10	9.30	7.65	7.90	9.50

In each of the six different $\text{PuO}_2(\text{CO}_3)_3^{4-}$ samples examined, two NMR signals are present, one for the free carbonate ligand and one for the carbonate ligand coordinated to a paramagnetic plutonium metal center. For the $\text{PuO}_2(\text{CO}_3)_3^{4-}$ system (Figure 3.2), the low field resonance at $\delta = 166$ ppm is assigned to the free carbonate ligand, and the high field resonance at $\delta = -210$ ppm is assigned to the $\text{PuO}_2(\text{CO}_3)_3^{4-}$ complex. Recall from Figure 3.1 that the $\text{PuO}_2(\text{CO}_3)_3^{4-}$ molecule is expected to have D_{3h} symmetry and hence a single carbonate carbon environment. The single ^{13}C resonance line for this species seen in Figure 3.2 is consistent with our expectations based on the solid state structure shown in Figure 3.1. The free carbonate resonance seen at $\delta = 166$ ppm is a singlet representing the fast exchange between uncomplexed carbonate and bicarbonate ions in solution (Patterson and Ettinger, 1962). Since the exchange between carbonate and bicarbonate is very fast on the NMR time-scale, it does not affect the exchange broadening of the $\text{PuO}_2(\text{CO}_3)_3^{4-}$ system. Below room temperature, the exchange reaction is slow on the actual time-scale (Figure 3.2). At higher temperature, a substantial line broadening is observed in the free carbonate signal, while little line broadening is observed in the NMR signal for the coordinated carbonate.

The relative values of the exchange life-time, τ_M , and paramagnetic relaxation time, T_{2M} , will determine the effect of the paramagnetic ion on the experimental line width. The temperature dependence of the free carbonate signal seen in Figure 3.2 reveals that chemical exchange is rate determining ($\tau_M > T_{2M}$) since the NMR signal experiences a steady line-broadening with increasing temperature, while for the coordinated carbonate signal, relaxation is dominant ($T_{2M} > \tau_M$). This is characterized by the lack of change in line-broadening of this signal with increasing temperature.

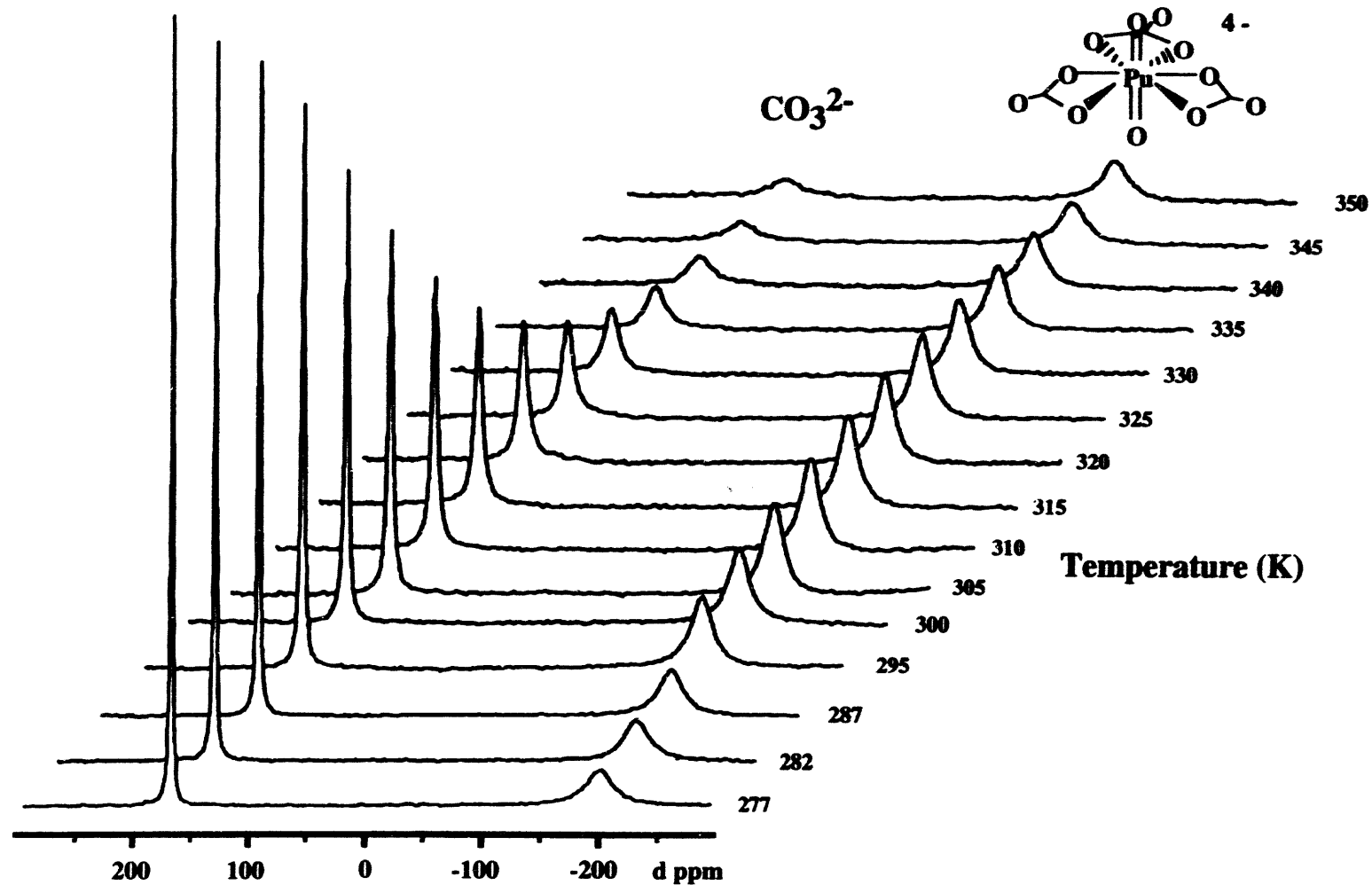


Figure 3.2. 62.9 MHz ^{13}C NMR spectra for solutions containing 99.9% ^{13}C -enriched $^{242}\text{PuO}_2(\text{CO}_3)_3^{4-}$ ($\delta = -209$ ppm at 25°C) and free carbonate (averaged signal for HCO_3^- and CO_3^{2-} , $\delta = 166$ ppm at 25°C) as a function of temperature. Solution conditions: $[\text{PuO}_2^{2+}] = 0.20\text{M}$; $[\text{CO}_3^{2-}] / [\text{HCO}_3^-] = [\text{ClO}_4^-] = 1.00\text{M}$; $\text{pH} = 9.50$ [16].

3.4 Kinetic Data Treatment

When the nuclei under examination in an NMR experiment can exist in two environments, one of which is close to a paramagnetic ion, then the paramagnetic contribution to relaxation is extremely useful for determining the exchange rate of the nuclei between the two environments. When a paramagnetic ion is dissolved in a solvent containing an excess of a complexing ligand, there will be, in principle, two resonance lines resulting from the two types of ligand, coordinated and noncoordinated. The paramagnetic species will broaden the signal due to the diamagnetic species (the free ligand) via the chemical exchange. The line will broaden as a function of exchange, and this behavior has been rigorously treated by Swift and Connick (1962).

In the Swift and Connick approach, the NMR transverse relaxation time T_2 and the chemical shift $\Delta\omega_s$ between free and coalesced ligand signals can be related to the mean lifetime τ_M of a ligand molecule bound to the paramagnetic metal ion by Equations 3.2 and 3.3.

$$\frac{1}{T_{2p}} = \left(\frac{1}{T_2} - \frac{1}{T_{2a}} \right) = \frac{P_M}{\tau_M} \left\{ \frac{\frac{1}{T_{2M}^2} + \frac{1}{\tau_M T_{2M}} + \Delta\omega^2_M}{\left[\frac{1}{T_{2M}} + \frac{1}{\tau_M} \right]^2 + \Delta\omega^2_M} \right\} + \frac{P_M}{T_{2os}} \quad (3.2)$$

$$\Delta\omega_s = P_M \left\{ \frac{\Delta\omega_M}{\left[\frac{\tau_M}{T_{2M}} + 1 \right]^2 + \tau_M^2 \Delta\omega^2_M} \right\} + \Delta\omega_{os} \quad (3.3)$$

In Equation 3.2, T_2 is the NMR transverse relaxation time, T_{2p} and T_{2a} are the transverse relaxation times in the presence (p) and absence (a) of a paramagnetic

component, τ_M , τ_L , P_M and P_L are the mean residence times (τ) and mole fractions (P) of the ligand coordinated to the metal (M) and in solution (L). The lifetimes and mole fractions are related by $\tau_M/\tau_L = P_M/P_L$.

The reduced linewidth ($1/T_{2p}$) shows a marked dependence on temperature which can be separated into four regions characterized by different predominant relaxation processes. This temperature dependence is illustrated in Figure 3.3. The region in Figure 3.3 where $\ln(1/T_{2p})$ is roughly proportional to the exchange rate ($1/\tau_M$) is often referred to as the slow exchange domain. In the region of slow exchange, $\Delta\omega^2_M \gg 1/T_{2M}^2$, and $1/\tau_M^2$, and Equation 3.2 simplifies to Equation 3.4. However, the temperature dependence of the

$$\frac{1}{T_{2p}} = \frac{1}{P_M} \left(\frac{1}{T_2} - \frac{1}{T_{2a}} \right) = \frac{1}{\tau_M} \quad (3.4)$$

coordinated carbonate signal seen in Figure 3.2 reveals that paramagnetic relaxation is the dominant process in the plutonium(VI) carbonate system at all temperatures under consideration. Thus the pseudo-first-order rate constant *cannot* be calculated from the coordinated carbonate signal in the usual manner, instead one must use the signal of the free carbonate ligand. Recall from Figure 3.2 that the free carbonate ligand signal does show an increase in line-broadening as a function of temperature. Thus substitution of $\tau_M/\tau_L = P_M/P_L$ into Equation 3.4 gives Equation 3.5 which can be used to measure the carbonate exchange rate by following the linewidth change in the free carbonate resonance.

$$\frac{1}{T_{2p}} = \frac{1}{P_L} \left(\frac{1}{T_2} - \frac{1}{T_{2a}} \right) = \frac{1}{\tau_L} = k_{ex} \quad (3.5)$$

Ideally the observed transverse relaxation rate, T_2 , is related to the NMR line width by $1/T_2 = \pi\Delta\nu_{1/2}$ where $\Delta\nu_{1/2}$ represents the full width at half the maximum height of the

NMR signal. Line widths of the broadened NMR signal are generally calculated from a Lorentzian linefit program. However, line widths are also affected by the magnetic field inhomogeneities due to the paramagnetic solutions, inadequate digitization, inhomogeneities of the static field, etc. Therefore, the interpretation of these line widths according to $1/T_2 = \pi\Delta\nu_{1/2}$ may lead to an overestimation of $1/T_2$ and thus to an underestimation of the exchange rate constant, k_{ex} . These potential problems have been avoided in the work reported here. First, the kinetic contribution to the relaxation parameters has been enhanced by the use of a high-field magnet (5.87 T). Second, a Carr-Purcell-Meiboom-Gill (CPMG) pulse sequence was applied for the experimental determination of $1/T_2$, thus avoiding the inhomogeneity problems noted above (Carr and Purcell, 1954; Meiboom and Gill, 1958).

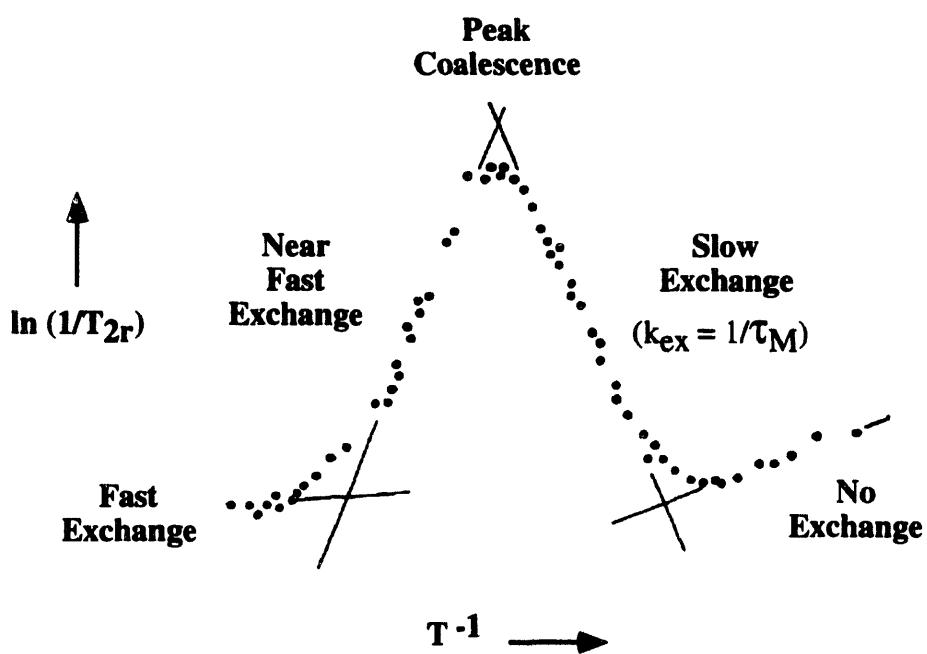


Figure 3.3. The influence of chemical exchange on the line width, $\Delta\nu_{1/2}$, of an NMR signal as a function of temperature.

In general, the relaxation times of paramagnetically-relaxed NMR signals are very short, so that short echo (τ) times are needed for the measurement of $1/T_2$ when using the CPMG pulse sequence. However, many routine spectrometers are limited in the choice of τ values by the software, and the shortest τ available may not allow for precise measurements of $1/T_2$ (i.e. not enough spin echoes will be observed for accurate determination of $1/T_2$). A modified CPMG pulse sequence was therefore written to overcome these software difficulties. A typical (CPMG) T_2 experiment is shown in Figure 3.4, where we are observing the decay of the free carbonate NMR signal intensity as a function of echo time τ . This decay is described by the exponential equation $I_0 = I_\tau \exp(-\tau/T_2)$ from which $1/T_2$ can be extracted by a curve-fitting procedure. In our experimental procedure, $1/T_{2a}$ for free carbonate ($[\text{CO}_3^{2-}] = [\text{ClO}_4^-] = 1\text{M}$) was measured using the CPMG pulse sequence over a wide temperature range and found to be relatively constant at 2.9 ± 0.2 Hz in the pH range under study. This free carbonate T_{2a} data is given in Table 3.2. Next a solution of paramagnetic PuO_2^{2+} ions in carbonate solution was studied over an equally wide temperature range. At each temperature, a complete pulsed NMR determination of $1/T_2$ was made, and the value of the reduced line width, $1/T_{2p}$, was calculated according to Equation 3.5. Typical data are shown in Tables 3.3 and 3.4 for plutonium concentrations of 0.1 and 0.2 M. Finally, since $1/\tau_L$ is a rate constant for a kind of chemical reaction, its temperature dependence may be obtained from transition-state theory (Equation 3.6), where k_b and h are Boltzmann's and Planck's constants, respectively, and R is the universal gas constant. The activation enthalpy (ΔH^\ddagger) and entropy (ΔS^\ddagger) were obtained from the Eyring relationship (Equation 3.6) and the resulting Eyring data is presented in Figure 3.5

$$\frac{1}{T_{2p}} = \frac{1}{\tau_L} = k_{\text{ex}} = \left(\frac{k_b T}{h}\right) \exp\left(\frac{\Delta S^\ddagger}{R} - \frac{\Delta H^\ddagger}{RT}\right) \quad (3.6)$$

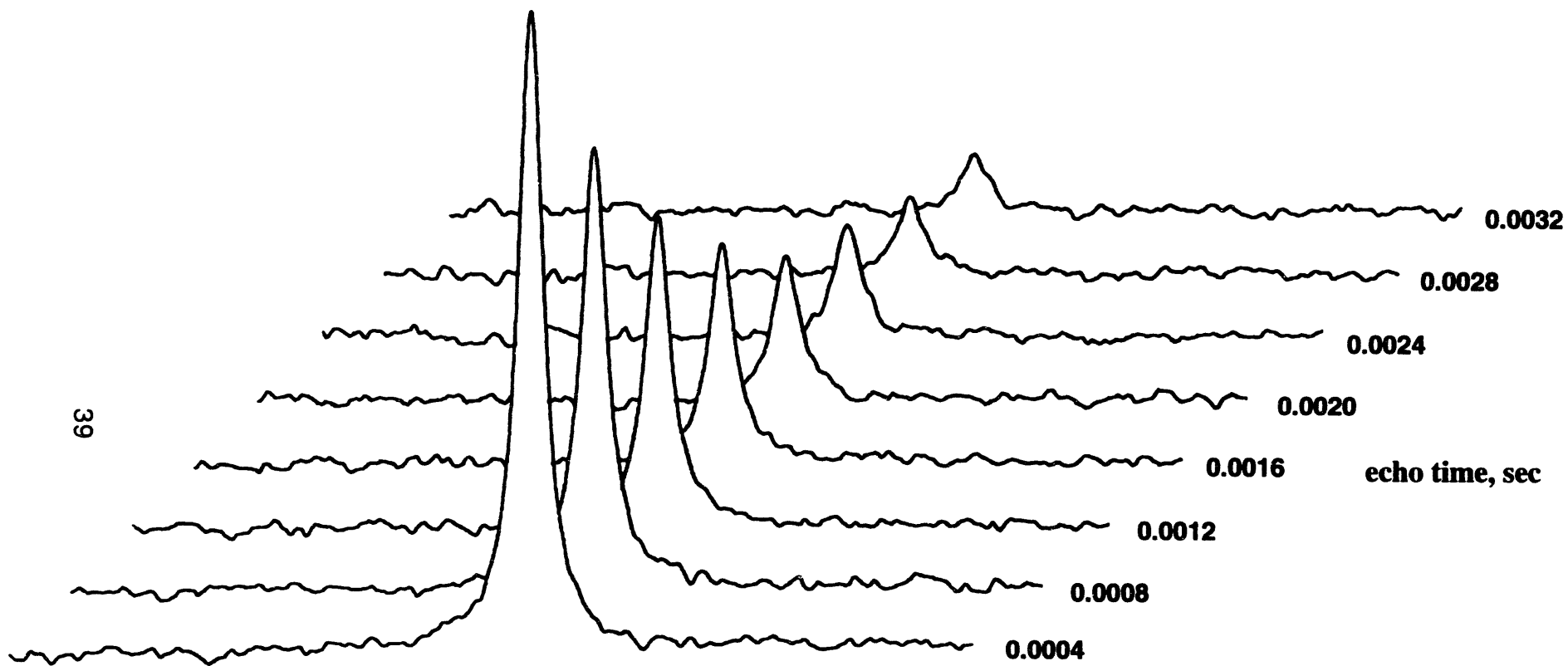


Figure 3.4. A typical ^{13}C NMR spin-echo relaxation experiment following the free carbonate resonance

Table 3.2. T_2 Spin-echo data^a for free carbonate under the following conditions: $[\text{CO}_3^{2-}] = 1.0\text{M}$; $[\text{ClO}_4^-] = 1.0\text{M}$; $\text{pH} = 10.18$

T_{obs}	T_{2a}	$1/T_{2a}$	$\Delta\nu_{1/2} = 1/\pi T_{2a}$
295K	0.35 s	2.860 Hz	0.910 Hz
300K	0.31 s	3.239 Hz	1.031 Hz
315K	0.36 s	2.744 Hz	0.873 Hz
320K	0.38 s	2.616 Hz	0.833 Hz
325K	0.34 s	2.977 Hz	0.948 Hz
330K	0.36 s	2.765 Hz	0.880 Hz
ave	0.35 (± 1) s	2.86 (± 0.1) Hz	0.91(± 0.1) Hz

T_{obs} = observed temperature in °C.

T_{2a} = Transverse relaxation rate in the absence of paramagnetic material

$\Delta\nu_{1/2}$ = full width a half the maximum height

Table 3.3. Plutonyl Carbonate Sample 1 Data

T_o	T_c	$1/T_{2a}$	$1/T_2$	ρ_L/T_{2p}	$k = 1/T_{2p}$	$\ln k$	$\ln(k/T)$	ρ_L
275	275.56	2.9	76.5	73.6	103.7	4.641	-0.977	0.71
280	280.51	2.9	103.7	100.8	142.0	4.956	-0.681	0.71
285	285.38	2.9	121.9	119.0	167.6	5.122	-0.532	0.71
290	290.26	2.9	178.9	176.0	247.9	5.513	-0.158	0.71
295	295.14	2.9	199.3	196.4	293.1	5.626	-0.007	0.71
300	300.02	2.9	268.7	265.8	408.9	5.925	0.310	0.71
315	314.65	2.9	500.0	497.1	801.8	6.551	0.935	0.71
320	319.53	2.9	640.7	637.8	1028.7	6.801	1.169	0.71
325	324.41	2.9	901.8	898.9	1449.8	7.144	1.497	0.71
330	329.29	2.9	1075.6	1072.7	1730.2	7.320	1.659	0.71
335	334.16	2.9	1344.1	1341.2	2163.2	7.544	1.868	0.71

^a Solution Conditions: $[\text{Pu}^{\text{VI}}] = 0.2M$, $[\text{CO}_3^{2-} + \text{HCO}_3^-] = 1.1M$, $\text{pH} = 9.48$

T_o = observed temperature in °C.

T_c = corrected temperature in °C.

T_2 = Transverse NMR relaxation rate

T_{2a} = Transverse NMR relaxation rate in the absence of paramagnetic material

T_{2p} = Transverse NMR relaxation rate in the absence of paramagnetic material

ρ_L = Mole fraction of free ligand.

Table 3.4. Plutonyl Carbonate Sample 2 Data^a

T_o	T_c	$1/T_{2a}$	$1/T_2$	ρ_L/T_{2p}	$k = 1/T_{2p}$	$\ln k$	$\ln(k/T_c)$	ρ_L
297	297.09	2.9	183.97	181.1	229.2	5.435	-0.259	0.79
302	301.97	2.9	232.83	229.9	291.0	5.673	-0.037	0.79
307	306.85	2.9	297.55	294.7	373.0	5.922	0.195	0.79
312	311.73	2.9	409.22	406.3	514.3	6.243	0.501	0.79
317	316.60	2.9	537.74	534.8	677.0	6.518	0.760	0.79
322	321.48	2.9	605.23	602.3	762.4	6.636	0.864	0.79
327	326.36	2.9	229.73	226.8	287.1	5.660	-0.128	0.79
332	331.24	2.9	836.73	833.8	1055.5	6.962	1.159	0.79

^a Solution conditions. $[\text{Pu}^{\text{VI}}] = 0.1M$, $[\text{CO}_3^{2-} + \text{HCO}_3^-] = 0.95M$, $\text{pH} = 10.10$

T_o = Observed temperature in °C.

T_c = Corrected temperature in °C.

T_2 = Transverse NMR relaxation rate

T_{2a} = Transverse NMR relaxation rate in the absence of paramagnetic material

T_{2p} = Transverse NMR relaxation rate in the absence of paramagnetic material

ρ_L = Mole fraction of free ligand.

The Eyring analysis shown in Figure 3.5 gives data for experimental measurements employing 0.1 and 0.2 M plutonium concentrations. The exchange rate constants (k_{ex}) are apparent first order rate constants and will depend on [Pu(VI)]. By assuming a first order dependence, the k_{ex} values can be divided by [Pu(VI)] to give second order rate constants. The fact that these constants all fall on a straight line supports the assumption. These second order rate constants are given in Table 3.5. The Eyring analysis at standard conditions provides activation parameters of $\Delta H^\ddagger = 38 \text{ KJ/M}$ and $\Delta S^\ddagger = -60 \text{ J/K}$ for the plutonyl triscarbonate system at 295K. These activation parameters are compared with literature values for other actinyl triscarbonate systems in Table 3.6. From Table 3.6 it can be seen that our activation parameters for plutonium (VI) extend those reported by Stout *et al.* (1992) for the uranyl and neptunyl triscarbonate systems, but are not consistent with those reported by Brücher *et al.* (1991) for the uranyl system. The origin of the discrepancy between activation parameters for uranium is not clear.

3.5 Mechanism of Carbonate Exchange

The classification of substitution reaction mechanisms originally proposed by Langford and Gray, and widely used in coordination chemistry, is based on operational criteria. If kinetic tests show the presence of an intermediate of increased coordination number, the mechanism is termed associative and labeled A. If an intermediate of reduced coordination number can be detected, the mechanism is called dissociative and labeled D. When no intermediate species can be found, the mechanism is declared a concerted interchange process, denoted I. Within this last category, a further distinction is made, depending on whether evidence can be found for important incoming group influences (I_a) or not (I_d).

In general the values of ΔH^\ddagger for each actinyl triscarbonate system are relatively small and positive, while the ΔS^\ddagger values are large and negative. The negative entropy is suggestive of a highly ordered or associative transition state. Similar parameters have also been reported for the acid-catalyzed aquation of bidentate carbonate complexes (Palmer and Van Eldik, 1983). The rate determining step in the aquation reaction mechanism involves protonation of the carbonate ligand, which opens a ring formed by one of the bidentate carbonates attached to the central metal ion. This is followed by rapid

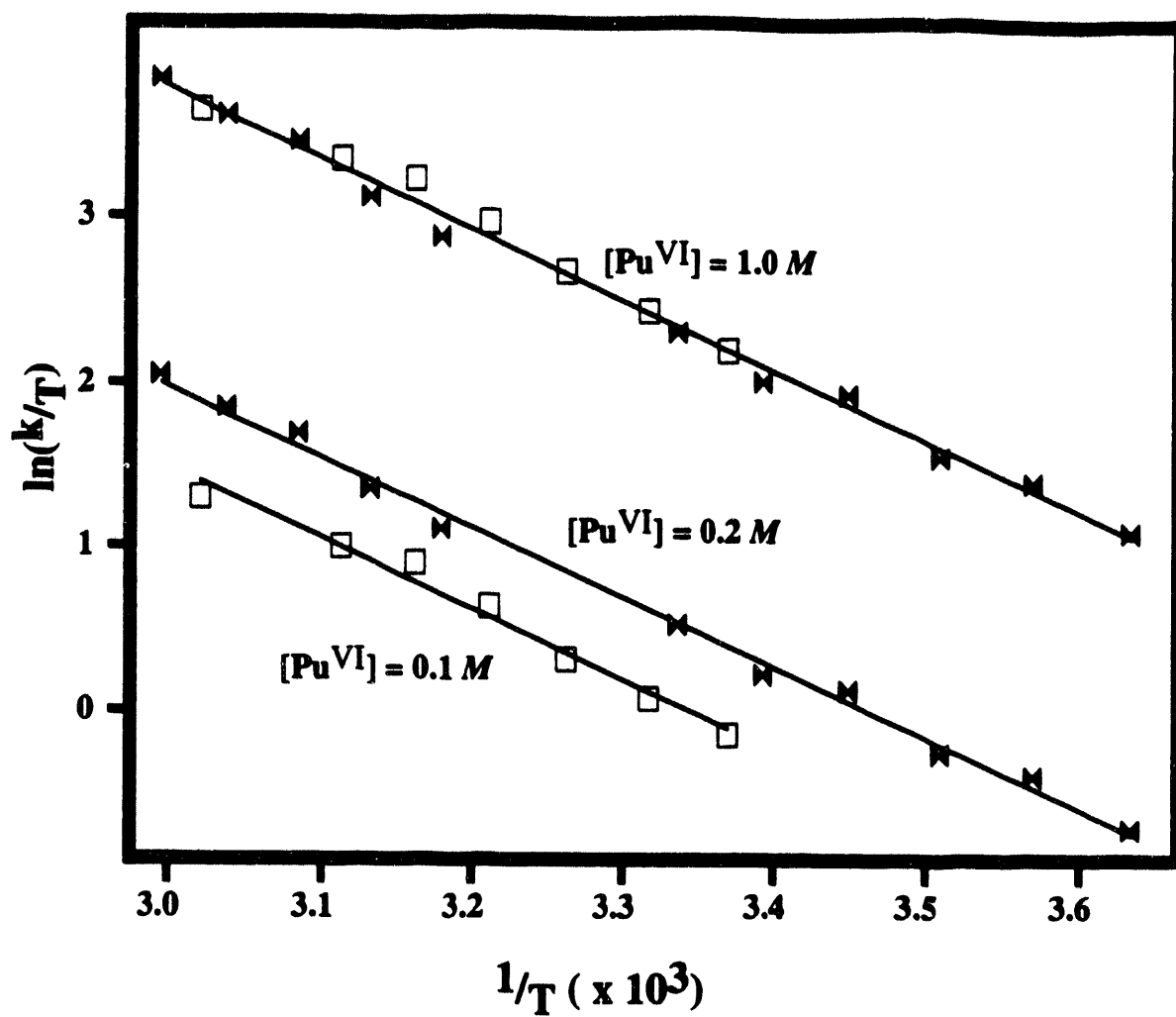


Figure 3.5. Eyring plots for the plutonyl tris carbonate system at plutonium concentrations listed.

Table 3.5. Plutonyl Carbonate Sample Data Corrected to 1M Concentration

T_o	T_c	$k = 1/T_{2p}$	T_o	T_c	$k = 1/T_{2p}$
275	275.56	809.7	307	306.85	4305.8
280	280.51	1108.9	312	311.73	5936.4
285	285.38	1309.1	317	316.60	7813.9
290	290.26	1936.2	320	319.53	7016.5
295	295.14	2160.6	322	321.48	8799.6
297	297.09	2645.8	325	324.41	9888.9
300	300.02	2924.1	330	329.29	11800.8
302	301.97	3359.0	335	334.16	14754.7
315	314.65	5468.6	332	331.24	12182.3

Table 3.6. Comparison of activation parameters for actinyl triscarbonate systems.^a

An	U	U	Np	Pu	
ΔH^\ddagger	82	53	42	35	KJ/M
ΔG^\ddagger_{295}	67	65	63	53	KJ/M
ΔS^\ddagger_{295}	50	-40	-70	-61	J/M-K
Transition State	D	A	A	A	
Reference	1	2	2	3	

^a D = Dissociative, A = Associative

- 1) Brücher, E.; Glaser, J.; Toth, I. *Inorg. Chem.*, **30** (1991) 2239.
- 2) B. E. Stout, G. R. Choppin, and J. C. Sullivan, "Exchange Studies of Actinyl Carbonate Complexes," to appear in the Proceedings of the Symposium to Commemorate the Fiftieth Anniversary of the Discovery of the Transuranium Elements, Washington D.C., August 27-29 (1990).
- 3) This work

dissociation of the monodentate bicarbonate species. We propose an analogous mechanism for carbonate exchange in all the actinyl triscarbonate systems (see Figure 3.6). In this mechanism, the addition of carbonate or bicarbonate (acid-catalyzed pathway) forms an intermediate activated complex $[An^{VI}O_2(CO_3)_4^{6-}]^\ddagger$ in which four carbonates are bound, two in a monodentate manner. Such a transition state is expected to be highly ordered with a negative entropy of activation. Protonation of this complex is followed by a rapid dissociation of bicarbonate and the reforming of a metal-oxygen bond by one of the monodentate carbonate ligands.

3.6 Concluding Remarks

In contrast to the many studies of ligand exchange on lanthanide ions, relatively little data has been reported for the corresponding ligand substitution kinetics of the actinide ions, with uranyl receiving by far the most attention. To the best of our knowledge, there are two reviews of ligand exchange reactions involving uranium (Lincoln, 1979; Tomiyasu and Fukutomi, 1982). For these reactions, mostly D or I_d mechanisms have been proposed for substitutions involving monodentate ligands, but there seems to be no conclusion in the literature regarding bidentate substitutions. Two rate laws have been observed for the ligand exchange process, the first being independent of the free ligand concentration [L] indicating a D mechanism, while the second obeys a two term rate law for which the observed pseudo-first order exchange rate constant may be expressed as $k_{ex} = k_1 + k_2[L]$. The k_1 term may be ascribed to a D type ligand exchange process in which a reactive intermediate with one less ligand is generated. The k_2 term is consistent with either an I_d mechanism under limiting conditions, or an associative (A) mechanism in which the rate determining step is the formation of a transition state in which the coordination number is increased by one. The usual test for an A mechanism whereby the dependence of the magnitude of k_2 upon the nature of the incoming group is observed is not possible for these

ligand exchange processes, and thus a definitive choice between A and I_c mechanism may not be possible.

For the lanthanide ions, the early, larger ions are characterized by relatively small enthalpies and very negative entropies of activation indicative of A or I_a mechanisms, whereas exchange involving complexes of the smaller, later lanthanide ions are characterized by much larger enthalpies and more positive entropies of activation, which are indicative of an activation process involving bond dissociation.

Our studies demonstrate that NMR spin-echo relaxation techniques are directly applicable to paramagnetic actinide complexes and will undoubtedly have a significant impact in the areas of actinide speciation and solution chemistry kinetics.

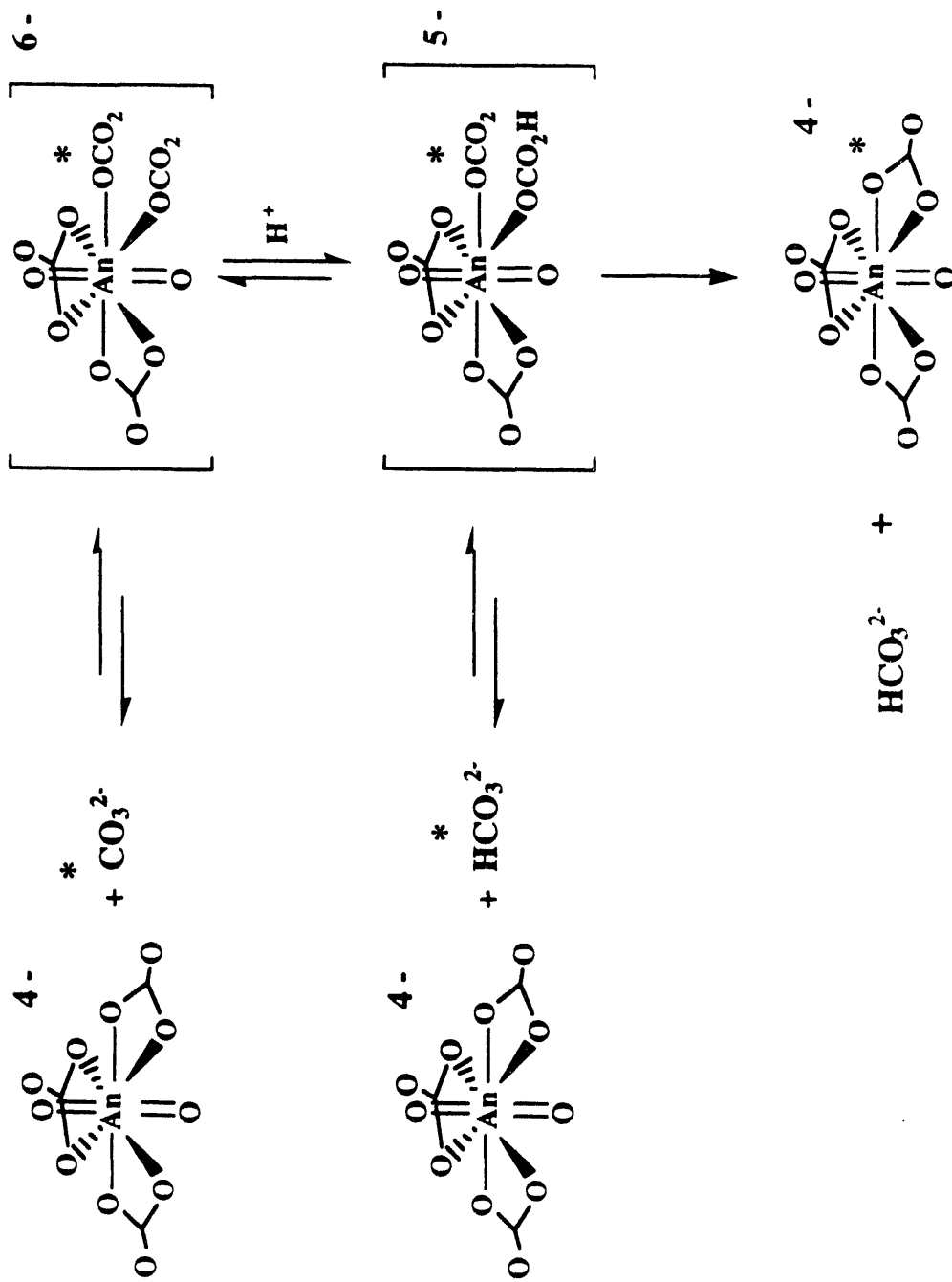


Figure 3.6. Proposed mechanism for carbonate self-exchange on actinyl tris carbonate complexes in aqueous solution.

4. Acknowledgments

We would like to thank Dr. D.E. Hobart for graciously supplying the ^{242}Pu used in this study, Dr. T.E. Newton for preparing the Pu-colloid samples used, and Drs. D. E. Wheeler and J. R. Brainard for helpful discussions.

This work was supported by the Yucca Mountain Site Characterization Project Office as part of the Civilian Radioactive Waste Management Program. This project is managed by the U.S. Department of Energy, Yucca Mountain Site Characterization Project.

5. References

Åberg, M., Ferri, D., Glaser, J., and Grenthe, I. (1983a). "Studies of Metal Carbonate Equilibria. 8. Structure of the Hexakis (carbonato) tris [dioxouranate(VI)] Ion in Aqueous Solution. An X-ray Diffraction and ^{13}C NMR Study," Inorganic Chemistry, Vol. 22, pp. 3981-3985. NNA.930707.0051

Åberg, M., Ferri, D., Glaser, J., and Grenthe, I. (1983b). "Structure of the Hydrated Dioxouranium(VI) Ion in Aqueous Solution. An X-ray Diffraction and ^1H NMR Study," Inorganic Chemistry, Vol. 22, pp. 3986-3989. NNA.940323.0282

Allard, B. (1982). "Solubilities of Actinides in Neutral or Basic Solutions," in Actinides in Perspective, N. Edelstein, ed., Pergamon Press, New York, pp. 553-580. NNA.891212.0007

Baes, C. F. and Mesmer, R. E. (1976). The Hydrolysis of Cations, J. Wiley and Sons, N. Y. HQS.880517.1945.

Basile, L. J.; Ferraro, J. R.; Mitchell, M. L.; Sullivan, J. C. "The Raman Scattering of Actinide(VI) ions in Carbonate Media" *Appl. Spectroscopy*. **1978**, 32, 535. NNA.940323.0277.

Beitz, J. V., Bowers, D. L., Doxtader, M. M., Maroni, V. A., and Reed, D. T. (1988). "Detection and Speciation of Transuranium Elements in Synthetic Groundwater Via Pulsed-Laser Excitation," Radiochimica Acta, Vols. 44-45, pp. 87-93. NNA.931214.0042

Bennett, D. A., Hoffman, D., Nitsche, H. Russo, R. E., Torres, R. A. Baisden, P. A. Andrews, J. E. Palmer, C. E. A., and Silva, R. J. (1992). "Hydrolysis and Carbonate Complexation of Dioxoplutonium(V)," Radiochimica Acta, Vol. 56, pp. 15-19. NNA920416.0043

Berg, J. M., Morris, D. E., Clark, D. L., Tait, C. D., Woodruff, W. H., and VanDer Sluys, W. G. (1991a). "Pulsed Photothermal Spectroscopy Applied to Lanthanide and Actinide Speciation," Proceedings of the SPIE, Vol. 1435, p. 331. NNA.940323.0283

Berg, J. M., Tait, C. D., Morris, D. E., and Woodruff, W. H. (1991b). "Actinide Speciation by Photothermal Spectroscopies: Instrumentation Development," Materials Research Society Symposium Proceedings, Vol. 212, p. 531. NNA.940124.0042

Brimhall, G. H. and Crerar, D. A. (1987). "Ore Fluids: Magmatic to Supragene." In Thermodynamic Modeling of Geological Materials: Minerals, Fluids, and Melts, I. S. E. Carmichael and H. P. Eugster (eds.), Reviews in Mineralogy Vol. 17, Mineralogical Society of America, pp. 255-321. NNA.940323.0287.

Brücher, E., Glaser, J., and Toth, I. "Carbonate Exchange for the Complex $\text{UO}_2(\text{CO}_3)_3^{4-}$ in Aqueous Solution as Studied by ^{13}C NMR Spectroscopy" (1991). Inorg. Chem. Vol. 30, p. 2239. NNA.930707.0052

Carnall, W. T. and Crosswhite, H. M. (1989). In The Chemistry of the Actinide Elements, J. J. Katz, G. T. Seaborg, and L. R. Morss (eds.), Ch. 15, Chapman-Hall, London. Readily available.

Carr, H. Y. and Purcell, E. M. (1954). "Effects of Diffusion on Free Precession in NMR Experiments" Phys. Rev., Vol.94, p. 630. NNA.940204.0001

Ciavatta, L.; Ferri, D.; Grimaldi, M.; Palombari, R.; Salvatore, F. "Dioxouranium(VI) Carbonate Complexes in Acid Solution" *J. Inorg. Nucl. Chem.* **1979**, *41*, 1175. NNA.931214.0047

Coda, A.; Della Giusta, A.; Tazzoli, V. "The Structure of Synthetic Andersonite, $\text{Na}_2\text{Ca}[\text{UO}_2(\text{CO}_3)_3] \cdot \text{H}_2\text{O}$ ($x \approx 5,6$)" *Acta. Cryst.* **1981**, *B37*, 1496. NNA.931214.0048

Combes, J. M., Chisholm-Brause, C. J., Brown, Jr., G. E., Parks, G. A., Conradson, S. D., Eller, P. G., Triay, I. R., Hobart, D. E., and Meijer, A. (1992). "EXAFS Spectroscopic Study of Neptunium(V) Sorption at the α -FeOOH / Water Interface," Environmental Science and Technology, Vol. 26, pp. 376-382. NNA.931214.0043

DOE (U.S. Department of Energy) (1988). "General Guidelines for the Recommendation of Sites for Nuclear Waste Repositories," Code of Federal Regulations, Energy, Title 10, Part 960, Washington, DC. NNA.900720.0050

DOE (U.S. Department of Energy) (1988). "Site Characterization Plan, Yucca Mountain Site, Nevada Research and Development Area, Nevada," DOE/RW-0199 Office of Civilian Radioactive Waste Management, Washington, DC. HQS.880517.2987

Eiswirth, M., Kim, J. I., and Lierse, C. (1985). "Optical Absorption Spectra of Pu(IV) Carbonate / Bicarbonate Media," Radiochimica Acta, Vol 38, pp. 197-201. HQS.880517.3074

Ferri, D., Glaser, J. and Grenthe, I. (1988). "Confirmation of the Structure of $(\text{UO}_2)_3(\text{CO}_3)_6^{6-}$ by ^{17}O NMR," Inorganica Chimica Acta, Vol. 148, pp. 133-134. NNA.940124.0037.

Fred, M. S. (1989). In The Chemistry of the Actinide Elements, J. J. Katz, G. T. Seaborg, and L. R. Morss (eds.), Ch. 16, Chapman-Hall, London. Readily available.

Hobart, D. E.; Samhoun, K.; Peterson, J. R. "Spectroelectrochemical Studies of the Actinides: Stabilization of Americium(IV) in Aqueous Carbonate Solution" *Radiochim. Acta*. **1982**, *31*, 139. NNA.940103.0070

Hobart, D. E. "Actinides in the Environment" in *Proceedings of the Robert A. Welch Foundation Conference on Chemical Research XXXIV: Fifty Years with Transuranium Elements*, Chapter XIII, Houston, TX, October 22-24, **1990**, 379. NNA.930405.0083

Hobart, D. E., Morris, D. E., and Palmer, P. D. (1989). "Formation, Characterization, and Stability of Plutonium(IV) Colloid: A Progress Report," Proceedings of the Topical Meeting on Nuclear Waste Isolation in the Unsaturated Zone: FOCUS '89, p. 118. NNA.940323.0286.

Kim, J. I., Lierse, C. Baumgartner, F. (1983). In Plutonium Chemistry, American Chemical Society Symposium Series, Vol. 216. Readily available.

Klenze, R. and Kim, J. I. (1988). "A Direct Speciation of Transuranium Elements in Natural Aquatic Systems by Laser-Induced Photoacoustic Spectroscopy," Radiochimica Acta, Vols. 44-45, pp. 77-85. NNA.931214.0041.

Koningsberger, D. C. and Prins, R., Eds. (1988). X-ray Absorption. Principles, Applications, Techniques of EXAFS, SEXAFS, and XANES, John Wiley and Sons, New York. Readily available.

Lincoln, S. F. "Dynamic NMR Studies of the Dioxouranium(VI) ion in Non-Aqueous Solution. Insights Into the Processes of Solvent and Ligand Exchange on Metal Ions in General" (1979). Pure Appl. Chem., Vol. 51, p. 2059. NNA.940124.0038.

Lindsay, W.L. (1979). Chemical Equilibria in Soil, John Wiley and Sons, New York. NNA.900214.0215

Madic, C.; Hobart, D. E.; Begun, G. M. "Raman Spectrometric Studies of Actinide(V) and -(VI) Complexes in Aqueous Sodium Carbonate Solution and of Solid Sodium Actinide(V) Ccarbonate Compounds" *Inorg. Chem.* **1983**, 22, 1494. NNA.940103.0067.

Martell, A. E. and Smith R. M. (1982). Critical Stability Constants, Volumes 1-5, Plenum Press, New York. Readily available.

Maya, L. "Hydrolysis and Carbonate Complexation of Dioxouranium(VI) in the Neutral-pH Range at 25 °C" *Inorg. Chem.* **1982**, 21, 2895. NNA.940103.0069.

Meiboom, S. and Gill, D.(1958). Rev. Sci. Inst., Vol. 29, p. 688. NNA.940124.0041.

Newton, T. W. and Rundberg, G. (1984). Materials Research Society Proceedings, Vol. 26, p. 867. HQS.880517.2028

Newton, T. W., Hobart, D. E. and Palmer, P. D. (1986a). "The Preparation and Stability of Pure Oxidation States of Neptunium, Plutonium, and Americium," Los Alamos National Laboratory Report No. LA-UR-86-967, Los Alamos, New Mexico. NNA.930406.0025

Newton, T. W., Hobart, D. E. and Palmer, P. D. (1986b). "The Formation of Pu(IV)-Colloid by the Alpha-Reduction of Pu(V) and Pu(VI) in Aqueous Solutions," Radiochimica Acta, Vol. 39, p. 139. NNA.920131.0408

Nitsche, H., Lee, S. C. and Gatti, R. C. (1987a). "Determination of Plutonium Oxidation States at Trace Levels Pertinent to Nuclear Waste Disposal," J. Radioanal. and Nucl. Chem., Vol. 124, No. 1, pp. 171-185. NNA.930326.0099.

Nitsche, H. (1987b). "Effects of Temperature on the Solubility and Speciation of Selected Actinides in Near-neutral Solution," Inorg. Chim. Acta, Vol. 127, pp. 121-128. NNA.940323.0284.

Nitsche, H., Müller, A., Standifer, E.M., Deinhammer, R.S., Becraft, K., Prussin, T., Gatti, R.C. (1992a). "Dependence of Actinide Solubility and Speciation on Carbonate Concentration and Ionic Strength in Groundwater," Radiochim. Acta, Vol. 58/59, p 27. NNA.940124.0043.

Nitsche, H., Gatti, R.C., and Lee, S.C. (1992b). "Low Level Determination of Plutonium by Gamma and L X-Ray Spectroscopy," Lawrence Berkeley Report, LBL-30617, J. Radioanal. Nucl. Chem., Vol 160, No. 2., NNA.930326.0092

Nitsche, H., Gatti, R.C., Standifer, E.M., Lee, S.C., Müller, A., Prussin, T., Deinhammer, R.S., Maurer, H., Becraft, K., Leung, S., and Carpenter, S.A. (1992c). "Measured Solubilities and Speciations of Neptunium, Plutonium, and Americium in a Typical Groundwater (J-13) from the Yucca Mountain Region," Milestone report M-3010, Yucca Mountain Site Characterization Project. U. S. Civilian Radioactive Waste Management Program. NNA.930507.0136.

Nitsche, H., Roberts, K. Prussin, T., Muller, A., Becraft, K., Keeney, D., Carpenter, S. A., and Gatti, R. C. (1992d). "Measured Solubilities and Speciations from Oversaturation Experiments of Neptunium, Plutonium, and Americium in UE25p#1 Well Water from the Yucca Mountain Region," Lawrence Berkeley Laboratory Report LBL-32897, Yucca Mountain Project Milestone Report 3329, in review. NNA.931015.0073.

Ogard, A. E., and Kerrisk, J. F. (1984). "Review of the Groundwater Chemistry along Flow Paths Between a Proposed Repository Site and the Accessible Environment," Los Alamos National Laboratory Report No. LA-10188-MS, Los Alamos, New Mexico. HQS.880517.2031

Okajima, S., Reed, D. T., Mazer, J. J., and Sabau, C. A. (1990). "Speciation of Pu(VI) in Near-Neutral to Basic Solutions Via Spectroscopy," Materials Research Society Symposium Proceedings, Vol. 176, pp. 583-590. NNA.931214.0040

Palmer, D. A. and Van Eldik, R. (1983) "The Chemistry of Metal Carbonate Complexes" Chem. Rev. Vol. 83, p. 651. NNA.940323.0285.

Patterson, P. and Ettinger, R. (1960). Z. Electrochem. Vol. 64, p. 98. NNA.940124.0045.

Pollard, P. M., Liezers, M., McMillan, J. W., Phillips, G., Thomason, H. P., and Ewart, F. T. (1988). "Some Actinide Speciation Using Laser Induced Photoacoustic Spectroscopy," Radiochimica Acta, Vols. 44-45, pp. 95-101. NNA.931214.0039.

Seward, T. M. (1984). "The formation of Lead(II) Chloride Complexes to 300°C: A Spectrophotometric Study," Geochimica et Cosmochimica Acta, Vol. 48, pp. 121-134. NNA.940124.0045.

Stout, B. E.; Choppin, G. R.; Sullivan, J. C. (1992) "The Chemistry of Uranium(VI), Neptunium(VI), and Plutonium(VI) in Aqueous Carboante Solutions" in Transactinide Elements. A Half Century, Morss, L. R.; Fuger, J. Eds, American Chemical Society, Washington, D. C., Chap. 23, 225. NNA.930707.0053

Strom, E. T., Woessner, D. E., and Smith, W. B. (1981). "¹³C NMR Spectra of the Uranyl Tricarbonate-Bicarbonate System," Journal of the American Chemical Society, Vol. 103, pp. 1255-1256. NNA.940124.0040.

Stumm, W., and Morgan, J. J. (1985). Aquatic Chemistry, 2nd Edition, John Wiley & Sons, New York, New York, pp. 171-229. HQZ.870301.1341

Stumpe, R., Kim, J. I., Schrepp, W., and Walther, H. (1984). "Speciation of Actinide Ions in Aqueous Solution by Laser-Induced Pulsed Photoacoustic Spectroscopy," Applied Physics B, Vol. 34, pp. 203-206. HQS.880517.2551

Swift, T. J. and Connick, R. E. "NMR Relaxation Mechanism of ^{17}O in Aqueous Solutions of Paramagnetic Cations and The Lifetime of Water Molecules in the First Coordination Sphere" (1962). J. Chem. Phys. Vol. 37, p. 307. NNA.931214.0046.

Tam, A. C. (1986). "Applications of Photoacoustic Sensing Techniques," Reviews of Modern Physics, Vol. 58, pp. 381 - 430. NNA.940124.0039.

Tomiyasu, H. and Fukutomi, H. (1982) "Kinetics of the Oxidation-Reduction and LIgand Substitution Reactions in Uranium Complexes". Bull. Res. Lab. Nucl. React. (Tokyo Inst. Technol.) Vol. 7, p. 57. NNA.931214.0045.

Triay, I. R., Hobart, D. E., Mitchell, A. J., Newton, T. W., Ott, M. A., Palmer, P. D., Rundberg, R. S., and Thompson, J. L. (1991). "Size Determination of Plutonium Colloid Using Autocorrelation Photon Spectroscopy," Radiochim. Acta, Vols. 52/53, pp. 127-131. NNA.930607.0060.

Ullman, W. J.; Schreiner, F. "Calorimetric Determination of the Enthalpies of the Carbonate Complexes of U(VI), Np(VI), and Pu(VI) in Aqueous Solution at 25 °C" Radiochim. Acta. 1988, 43, 37. NNA.940103.0068.

Wester, D. W. and Sullivan, J. C. (1983). "The Absorption Spectra of Pu(VI), (V), and (IV) Produced Electrochemically in Carbonate-Bicarbonate Media," Radiochem. Radioanal. Letters, Vol. 57, pp. 35-42. NNA.931214.0044.

Wolery, T. J. (1983). EQ3NR. A Computer Program for Geochemical Aqueous Speciation Solubility Calculations: User's Guide and Documentation, Lawrence Livermore National Laboratory, Livermore, CA, UCRL-53414. HQS.880517.2912

Wolery, T. J., Jackson, K. T., Boureier, W. L., Bruton, C. J., Viani, B. E., Knauss, K. G., and Delany, J. M. (1989). "The EQ3/6 Software Package for Geochemical Modeling: Current Status," Am. Chem. Soc. Symposium Volume, Chemical Modeling in Aqueous Systems II, pp. 105-116. HQX.891130.0044

6. Quality Assurance Documentation

Data in this paper is documented in laboratory notebooks TWS-INC-11-06-90-08, TWS-INC-11-06-91-06, TWS-INC-11-07-91-02, and TWS-INC-11-12-89-01. Because some of the software used for data collection / manipulation has not been officially sanctioned by the Yucca Mt. Site Characterization Project QA program, the data presented here may be non-quality affecting for the project. Preassigned accession number NNA.931015.0074.

DATE

FILMED

10/12/94

END

